From the Department of Oncology and Pathology
Karolinska Biomics Center
Karolinska Institutet, Stockholm, Sweden

INDUCTION AND REPAIR OF DNA DOUBLE-STRAND BREAKS IN HUMAN CELLS EXPOSED TO DIFFERENT RADIATION QUALITIES

Irina Radulescu

Stockholm 2008

Doctoral thesis
Induction and repair of DNA double-strand breaks in human cells exposed to different radiation qualities

All previously published papers were reproduced with permission from the publisher.
Published by Karolinska Institutet. Printed in Sweden by Universitetstryckeriet, Uppsala.
© Irina Radulescu, 2008
ISBN 978-91-7357-521-8

To my mother, Maria-Venera

ABSTRACT

Radiation therapy is used in attempting to kill tumor cells by inducing DNA double-strand breaks (DSB), the most critical DNA lesions. Recent and planned radiation therapy strategies use high-linear energy transfer (LET) radiation to effectively treat malignant tumors. The aim of this thesis was to investigate the mechanisms of DNA DSB induction and repair after exposure to ionizing radiation of different ionization densities, with focus on the role of DNA damage clustering and chromatin structure, as well as the activation of repair-related proteins at clustered damage sites in human cells.

DSB induction was assessed after exposure to accelerated ions of different ionization densities with LET ranging from 40 eV/nm to 300 eV/nm. Exposure of human cells to high-LET radiation resulted in clustering of DSB, leading to an excess of small DNA fragments (< 1 Mbp), as measured by pulsed-field gel electrophoresis (PFGE). Importantly, it was found that DNA organization into chromatin fibers and higher-order structures is responsible for most of DSB clustering induced by high-LET radiation.

A newly developed cold lysis protocol for preparation of genomic DNA, which avoids release of heat-labile sites (HLS) into DSB at elevated temperatures, was used to accurately measure the DSB number. DSB yields and relative biological effectiveness (RBE) values were strongly influenced by chromatin compactness. Furthermore, the presence of HLS had a substantial impact on DSB induction yields and DSB rejoining rates measured by PFGE. The lesions involved in the release of HLS into DSB were repaired independent of DNA-PKcs, XRCC1 or PARP-1. Moreover, cells with defect or inhibited function of DNA-PKcs did not show any fast rejoining of DSB when HLS were eliminated.

The substructure and spatial dynamics of DNA damage and repair along high-LET particle tracks was monitored by immunofluorescence. Interestingly, high-LET ion track irradiation revealed one of the earliest responses to ionizing radiation, ATM phosphorylation at Ser1981, as pATM foci that clearly correlated with γ-H2AX foci within particle tracks, as well as punctuated/diffuse staining dispersed throughout the whole nucleoplasm, far away from DSB. In addition, the number of γ-H2AX foci detected at early time-points was independent of the number of DSB, indicating that a single γ-H2AX focus contains clusters of several DSB within 1-2 Mbp of chromatin.

In summary, the presented data show that DSB yields and distributions are greatly influenced by ionization density and chromatin compactness. Clustering of DSB and other DNA lesions may affect the reparability. Furthermore, detection of protein activation in single cells after ion track irradiation suggested that chromatin changes or other signalling processes might take place at distance from DSB. This thesis provides new insights on the importance of the chromatin organization and the repair of clustered DNA damage sites, as well as the role of repair-associated proteins in DNA damage recognition after high-LET radiation.

Keywords: DSB; chromatin structure; high-LET; heat-labile sites; PFGE; DNA-PKcs; XRCC1; PARP-1; pATM; γ-H2AX; 53BP1.

ISBN 978-91-7357-521-8

LIST OF PUBLICATIONS

I. **Stenerlöw, B., Höglund, E., Elmroth, K., Karlsson, K. H. and Radulescu, I.,** Radiation quality dependence of DNA damage induction. *Radiation Protection Dosimetry*, 99, 137-141 (2002).

II. **Radulescu, I., Elmroth, K. and Stenerlöw, B.,** Chromatin organization contributes to non-randomly distributed double-strand breaks after exposure to high-LET radiation. *Radiation Research*, 161, 1–8 (2004).

III. **Karlsson, K. H., Radulescu, I., Rydberg, B. and Stenerlöw, B.,** Repair of radiation-induced heat-labile sites is independent of DNA-PKcs, XRCC1 or PARP (*Radiation Research*, 2008, in press).

IV. **Radulescu, I., Viktorsson, K., Qvarnström, O. F., Simonsson, M., Karlsson, K. H., Lewensohn, R. and Stenerlöw, B.,** ATM phosphorylation and formation of repair protein foci at clustered DNA damage sites (submitted).

CONTENTS

1 BACKGROUND……..……..1

1.1 CARCINOGENESIS AND CANCER THERAPY……..……...1

1.2 IONIZING RADIATION……..1

1.2.1 Tumor therapy using high-LET ion beams.....2

1.2.2 Low- versus high-LET radiation……3

1.3 CHROMATIN ORGANIZATION INSIDE THE CELL NUCLEUS..…5

1.4 EARLY SIGNALING OF DNA DOUBLE-STRAND BREAKS……...6

1.4.1 Early chromatin decondensation, MRN complex and ATM activation….....6

1.4.2 Phosphorylation of H2AX and recruitment of repair proteins at DNA DSBs……7

1.5 DNA DOUBLE-STRAND BREAK REPAIR……..8

1.5.1 NHEJ……..……...8

1.5.2 HR……...……..……10

2 THE PRESENT STUDY……..……..11

2.1 AIMS……...11

2.2 MATHERIALS AND METHODS……12

2.2.1 Cell cultures and inhibitors……..……12

2.2.2 Description and preparation of the chromatin structures……12

2.2.3 Irradiation……...13

2.2.4 Pulsed-field gel electrophoresis (PFGE) and DSB analysis…….....15

2.2.5 Immunofluorescence detection and analysis of foci…….16

2.3 SUMMARY OF THE PAPERS……..…17

2.3.1 Paper I……17

2.3.2 Paper II……..……..18

2.3.3 Paper III……..……18

2.3.4 Paper IV……..……..……19

2.4 DISCUSSION AND CONCLUSIONS……20

2.4.1 High-LET radiation induce a significant non-random distribution of DNA fragments ……..…20

2.4.2 Chromatin organization is responsible for non-random distribution of DSB after high-LET radiation ……..……..21
2.4.3 DSB yields and RBE values vary strongly when the chromatin structure becomes more open and the proteins are extracted ……..23
2.4.4 Heat-labile sites (HLS) affect the fast component of DSB rejoining……...23
2.4.5 Heat-released DSB are repaired independent of DNA-PKcs, XRCC1 or PARP-1..……..24
2.4.6 ATM phosphorylation is independent of the localization and level of DNA damage ……25
2.4.7 Single foci of γ-H2AX, MRE11 and 53BP1 may represent clusters of DSBs ……27
2.5 GENERAL CONCLUSIONS ……29
2.6 FUTURE STUDIES……29
3 ACKNOWLEDGEMENTS……...31
4 REFERENCES…… 33

LIST OF ABBREVIATIONS

53BP1	p53-binding protein 1
ATM	Ataxia-telangiectasia mutated
BRCA1/2	Breast cancer susceptibility protein 1/2
CHK1/2	Checkpoint kinase 1/2
DNA	Deoxyribonucleic acid
DNA-PKcs	DNA-dependent protein kinase catalytic subunit
DSB	Double-strand break
EDTA	Ethylenediaminetetraacetic acid
FAR	Fraction of activity released
H2AX	Histone 2A variant X
HLS	Heat-labile site
HR	Homologous recombination
LET	Linear energy transfer, measured in keV/μm or eV/nm
kbp	Kilobase pair
Mbp	Megabase pair
MDC1	Mediator of DNA damage checkpoint 1
MRE11	Meiotic recombination 11
MRN	MRE11/RAD50/NBS1 complex
NBS1	Nijmegen breakage syndrome 1
NHEJ	Non-homologous end joining
OER	Oxygen enhancement ratio
PARP-1	Poly(ADP-ribose) polymerase-1
pATM	Phosphorylated ATM
PFGE	Pulsed-field gel electrophoresis
RBE	Relative biological effectiveness
RPA	Replication protein A
SSB	Single-strand break
ssDNA	Single-stranded DNA
XLF	XRCC4-like factor
XRCC1/2/3/4	X-ray cross-complementary 1/2/3/4
γ-H2AX	Phosphorylated H2AX

1 BACKGROUND

1.1 CARCINOGENESIS AND CANCER THERAPY

Cancer is a disease characterized by cell aggressiveness (uncontrolled growth and division), invasiveness (invasion of normal tissues), and eventually metastasis (spreading to distant locations in the body).

Carcinogenesis is a process that consists of multistep mutations (changes in genomic DNA) starting with acquired abnormalities in genes, which can be inherited or appeared as a result of exposure to environmental factors. Such exposure may generate DNA lesions that lead to mutations, which may cause genomic instability. The development of a tumor (malignant growth) depends on several essential molecular alterations: self-sufficiency in growth signal, insensitivity to growth –inhibitory signals, avoidance of apoptosis, unlimited replicative potential, sustained angiogenesis, and tissue invasion and metastasis (Hanahan and Weinberg, 2000).

Current strategies for cancer therapy include surgery, radiation therapy, chemotherapy, immunotherapy, targeted therapy or a combination of these. When opting for a certain therapy, the tumor type and location, the stage of the disease, as well as the general status of the patient are to be considered. The aim of the treatment is the complete removal of cancer cells, with minimum damage to the normal tissues. The effectiveness of cancer therapy is often limited by adjacent tissue invasion or distant metastasis (for surgery), toxicity to the whole body (for chemotherapy), or by normal tissue damage (for radiotherapy). In addition, the tumor heterogeneity leads to survival of some resistant tumor cells, which increases the risk for recurrence and metastasis.

Radiation therapy uses ionizing radiation to damage the genetic material of cancer cells, making it impossible for them to continue to grow and divide. Radiation damages both cancer and normal cells, but most normal cells can recover from the effects of radiation and function properly. Radiation therapy aims to kill the tumor cells, while limiting the injury to the adjacent healthy tissue.

1.2 IONIZING RADIATION

Ionizing radiation is energetic particles or electromagnetic radiation that transfer their energy when interacting with matter, causing ionizations (*i.e.* emission of electrons from atoms). Examples of ionizing radiation are photons, electrons, neutrons and alpha particles. Charged particles such as electrons and alpha particles interact strongly with electrons, delivering their energy directly and producing ionizations along the particle track. In contrast, high-energy photons or neutrons are indirectly ionizing the matter by transferring their energy to charged particles, which, in turn, deliver the energy to the matter as above.

In a large number, the ionizations induced by radiation can be harmful to biological organisms, and can cause DNA damage in individual cells. On DNA level, the damage induced by ionizing radiation consists of single-strand breaks (SSBs),

double-strand breaks (DSBs), base damages, sugar damages, DNA-DNA and DNA-protein cross-links, as well as heat- and alkali-labile sites (revealed as strand breaks after alkaline or heat treatment of irradiated DNA) (Ward, 1988). If left unrepaired, the most critical lesion, the DSB, is related to cell death, chromosomal aberrations and genomic instability (Bryant, 1985; Burma et al., 2006; Goodhead, 1989). Therefore, accidental exposure to ionizing radiation may be lethal or lead to cancer development. Nevertheless, photons, electrons and more recently, heavy charged particle beams are used to treat malignant tumors. The damage on DNA is caused by direct or indirect actions of radiation, the latter appearing as a result of the water radiolysis, that forms free radicals (e.g. hydroxyl) which then induce lesions on DNA. Radiation therapy works by damaging the DNA of cells, and due to their higher cell-cycle turnover, cancer cells generally have a reduced capacity to repair the sub-lethal damage, compared to normal differentiated cells.

Radiation quality is a term used to describe different ionization densities produced by ionizing radiation delivering its energy to the matter. Linear energy transfer (LET) is a measure of the ionization density, and the LET concept is defined as the energy transferred per unit length of particle track, in eV/nm (Hall and Giaccia, 2006). The local complexity of clustered DNA lesions tends to increase with increasing LET, and high-LET radiation has a higher biological efficiency than low-LET radiation.

1.2.1 Tumor therapy using high-LET ion beams

Charged-particle therapy, such as proton therapy and carbon-ion therapy, is currently used to treat patients with deep-seated tumors. Compared to conventional radiation therapy with X-rays or gamma rays, the advantage of using protons and heavier particles for tumor therapy, is the excellent dose distribution that allows a high energy deposit within the tumor target volume, while minimizing the dose delivered to the surrounding healthy tissues (*Figure 1*). The heavy charged particles lose their energy at a higher rate when they reach the end of their range, with the peak of energy loss and highest dose delivered to the tissue at zero particle motility (the Bragg curve). This increased ionization results in a higher DNA damage in the Bragg peak region where the tumor is located, leaving a relatively lower risk of genetic mutations in normal tissue. This interesting characteristic of the dose-depth distribution is illustrated in *Figure 1*. However, the sharp Bragg peak needs to be spread out, to cover a volume of typical tumor dimensions. This can be accomplished by varying absorbers in front of the beam, resulting in beams of different energy which sum up forming a plateau with a uniform dose over the target tumor volume.

One of the limitations of radiotherapy is that the cells of solid tumors become deficient in oxygen. The hypoxic tumor cells are more resistant to radiation because oxygen makes permanent the damage produced by radiation induced free radicals. The oxygen enhancement ratio (OER), defined as the ratio of hypoxic to aerated doses to produce the same biological effect, decreases with increasing LET (Hall and Giaccia, 2006). Therefore, high-LET radiotherapy may overcome the resistance of hypoxic tumor cells encountered when using conventional radiotherapy. Another advantage of high-LET radiotherapy is the high relative biological effectiveness (RBE) for cell death

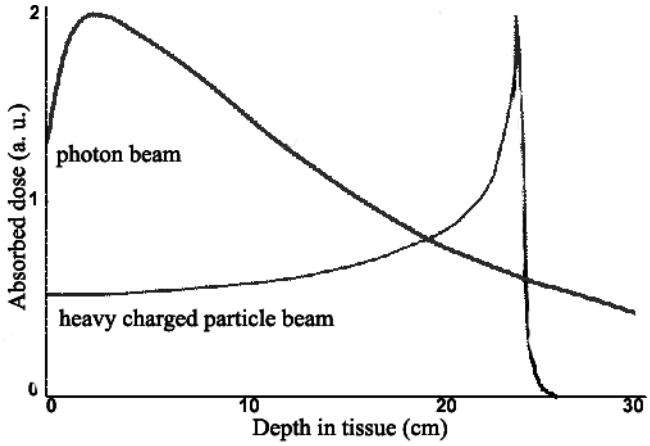

Figure 1. Typical dose-depth distribution for a heavy charged particle beam traversing a material (the Bragg curve) and for a photon beam.

as an endpoint. In summary, high-LET ion radiotherapy offers additional benefits such as a decreased dependence on oxygen status of the tumor, reduced repair capacity, less variation in sensitivity with the cell cycle, and high relative biological effectiveness, in addition to the excellent dose-depth distribution (Hall and Giaccia, 2006).

Recent and planned radiation therapy modalities use high-LET radiation, in terms of accelerated ions or radioactive nuclides emitting α-particles, to effectively treat malignant tumors. The cell killing efficiency of high-LET radiation could give a therapeutic advantage. However, the molecular events transferring a DSB into a dead cell are still unknown. Thus, studies of DSB induction and repair in relation to radiation quality could help identifying critical steps of this process.

1.2.2 Low- versus high-LET radiation

Ionization density influences the damage distribution in the genome. On the cellular level, low-LET radiation, such as X-rays and gamma radiation, induces sparsely ionizations which are typically randomly distributed within the nucleus (*Figure 2*). For such radiation, the predominant indirect action via free radicals can cause clusters of ionizations that lead to complex DSBs critical for cell survival (Goodhead, 1994). However, most of the DNA damage induced by low-LET radiation consists of SSB and base damages which are relatively easily repaired; a X-ray dose of 1 Gy induces about 1000 base damages, 1000 SSB and 40 DSB per cell nucleus (Goodhead, 1994; Hall and Giaccia, 2006).

In contrast to sparsely ionizing radiation, high-LET radiation (e.g. ions, alpha particles) leads to the induction of more complex and highly localized DNA damage along particle tracks (Goodhead, 1994; Hoglund and Stenerlow, 2001; Lobrich et al., 1996; Rydberg, 1996). Thus, high-LET induced DNA damage is a clustered lesion consisting of multiple strand breaks, base alterations etc., produced by the direct

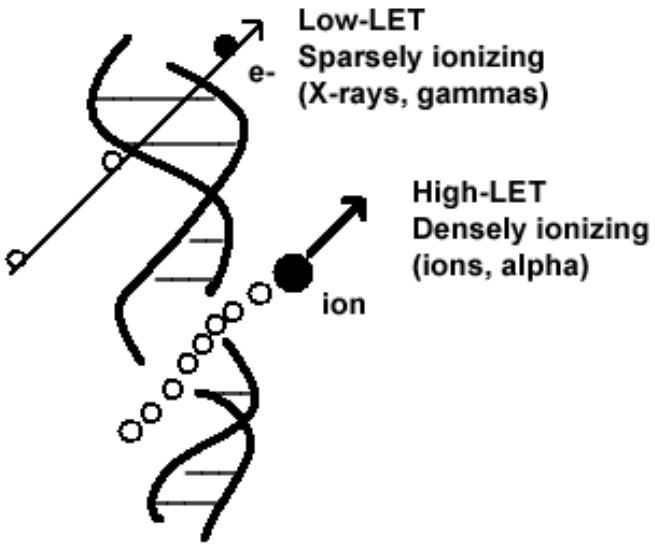

Figure 2. Effects of low- and high-LET radiation on DNA level. Low-LET radiation induces sparsely localized ionizations, which are randomly distributed within the nucleus. In contrast, high-LET ions are producing clusters of DNA lesions, as a result of the dense ionizations formed along the particle tracks.

interaction between DNA and the charged particle, which deposits its energy densely along its path (*Figure 2*). For the same radiation dose, the number of induced DSBs is only slightly higher after exposure to high-LET radiation, compared to photon exposure (Hoglund et al., 2000), but a DSB induced by high-LET radiation is 3-10 times more efficient in causing mutations or cell death (Cox et al., 1977). Both the localization and the complexity of high-LET induced DSB may influence the cellular capacity to repair such damage. The DNA damage induced by charged particles is associated with slower rejoining of DSBs (Lobrich et al., 1998; Pinto et al., 2005; Stenerlow et al., 1996), more complex mutations (Malyarchuk et al., 2004) and chromosomal instability (Singleton et al., 2002), as well as a larger fraction of γ-H2AX foci persistent 8-24 h post-irradiation (Karlsson and Stenerlow, 2004), when compared with the response after low-LET radiation. The DSBs are randomly distributed in cells exposed to low-LET radiation (Hoglund et al., 2000; Lobrich et al., 1998). In contrast, the dense ionizations along the charged particle tracks lead to the production of non-randomly distributed DSBs in intact cells, detected as an excess of DNA fragments smaller than 1 Mbp (Hoglund et al., 2000; Hoglund and Stenerlow, 2001; Lobrich et al., 1996; Newman et al., 1997; Rydberg, 1996). The traversal of a charged-particle track through the chromatin fiber produces clustering of DSB, and the non-random DNA fragmentation is probably influenced by the chromatin organization and track structure (Cucinotta et al., 2000; Hoglund and Stenerlow, 2001; Rydberg, 2001), although no direct evidence supported this hypothesis.

1.3 CHROMATIN ORGANIZATION INSIDE THE CELL NUCLEUS

In eukaryotic cells, compaction of the genome into chromatin fibers is essential to fit more than a meter long DNA double helix inside the cell nucleus of 10μm in diameter.

The basic unit of chromatin, the nucleosome, consists of 146 base pairs (bp) of DNA wrapped around a core histone octamer, which contains two copies of histones H2A, H2B, H3, and H4 (*Figure 3*) (Luger et al., 1997). Each histone consists of two domains, a histone fold domain that mediates the histone–histone and histone–DNA interactions important for building of the nucleosome, and a flexible amino-terminal tail domain. In addition, H2A and H2B have a carboxy-terminal tail domain (Downs et al., 2007). The tail domains contain sites for various histone post-translational modifications, which are shown to be a critical step in controlling the eukaryotic genomes by condensing and decondensing the chromatin (Ito, 2007). The enzymatic modification of histone tails controls the binding of ATP-dependent chromatin remodeling factors (e.g. RSC, SWI/SNF, INO80), which have the ability to alter histone-DNA contacts (Chai et al., 2005; Flaus et al., 2006). This, in turn, influences the level of chromatin compaction by the sliding of the nucleosomes on DNA, the removal of the histone octamer from DNA and other structural changes (Shim et al., 2007).

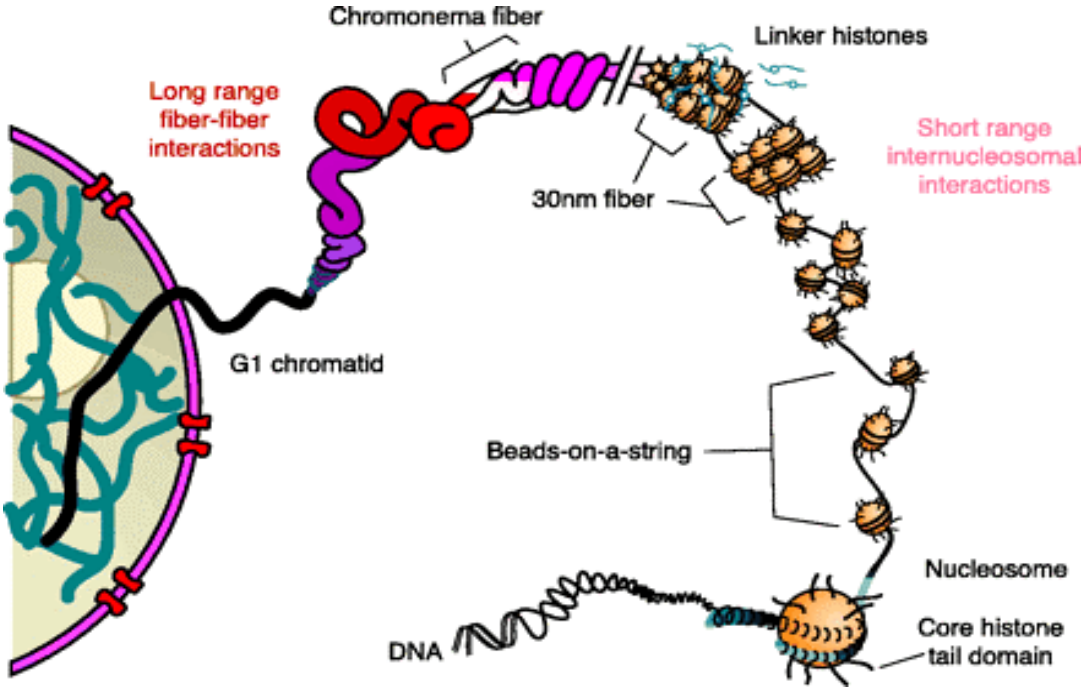

Figure 3. Chromatin organization inside the cell nucleus. Chromatin folding inside the the interphase nucleus occurs through various histone-dependent interactions, leading from the nucleosome unit, "beads-on-a-string" structure, to 30-nm chromatin fiber. This figure is reproduced with the author's permission. (Hansen, 2002; Horn and Peterson, 2002)

In addition, the level of chromatin compaction is also influenced by the binding of linker histones H1 and high-mobility group proteins (Downs et al., 2007). Linker histones also contain a globular domain essential for stabilizing the nucleosome structure and an amino- and a carboxy-terminal tail domains, proposed to be involved in chromatin folding (Horn and Peterson, 2002; Parseghian and Hamkalo, 2001; Ramakrishnan, 1997). The binding of linker histones leads to the formation of "beads-on-a-string" structure, and further folding through histone tail–mediated nucleosome-nucleosome interactions produces the 30-nm chromatin fiber (*Figure 3*). The organization of higher order chromatin structure further than the 30-nm fiber, and how the chromatin fiber is folded inside the nucleus, are issues still under investigation.

When DNA damage occurs, the higher-order chromatin folding represents a hinder to the detection and initiation of repair. Recent studies showed that DSB produce a local decondensation of the chromatin, as well as histone octamer removal and nucleosomes relocation on DNA (Kruhlak et al., 2006a; Shim et al., 2007). Moreover, DSB induction also results into post-translational modifications of the histone tails, such as the phosphorylation of the histone variant H2AX. Phosphorylated H2AX (γ-H2AX) spreads within seconds over a DSB flanking chromatin region, comprising of several kilobasepairs up to megabasepairs (Rogakou et al., 1999).

1.4 EARLY SIGNALING OF DNA DOUBLE-STRAND BREAKS

The human genome is constantly exposed to endogenous agents, such as free radicals generated during metabolic processes, and exogenous agents, such as ionizing radiation and chemicals. This exposure threatens the genome integrity and requires efficient mechanisms that attempt to alleviate or eliminate the DNA damage. To prevent a lethal or mutagenic propagation of the DNA lesion during cell division and to allow time to repair the damage, the DNA damage checkpoint arrests the cell cycle (Rouse and Jackson, 2002; Zhou and Elledge, 2000). If the damage is too complex to be efficiently repaired, the cell could undergo programmed cell death (Bree et al., 2004).

1.4.1 Early chromatin decondensation, MRN complex and ATM activation

Many aspects of DNA damage response initiation, including sensors involved and their interactions, are not fully understood. The early activation and recruitment to the damage sites of the protein kinase Ataxia-telangiectasia mutated (ATM), play a major role in signalling the DSB response pathways (Kastan and Lim, 2000). In connection to that, two models have been recently suggested. One hypothesis proposes that the MRN complex (consisting of NBS1, Rad50 and MRE11 proteins) is the first to arrive at the damaged site and is required both for activation of ATM and for initial recruitment of activated ATM to the damaged site (Dupre et al., 2006; Lee and Paull, 2005). After ATM activation and localization at DSBs, ATM autophosphorylates (Lee and Paull, 2005; You et al., 2005). In the second model, ATM is activated at distance from DSBs due to local changes in chromatin conformation (Bakkenist and

Kastan, 2003), prior to its recruitment to DSBs. ATM is activated by autophosphorylation on Ser1981 and dissociation of dimeric ATM (Bakkenist and Kastan, 2003), as well as recently identified autophosphorylation on Ser367 and Ser1893 (Kozlov et al., 2006).

The local chromatin decondensation initially restricted to the DSB site (Kruhlak et al., 2006a; Kruhlak et al., 2006b) has been shown to spread throughout the nucleus by an ATM-dependent pathway (Ziv et al., 2006), and this chromatin remodeling facilitates the access of repair proteins to DSBs. Active ATM phosphorylates various substrates which trigger cell cycle arrest and DNA repair. In addition to being downstream phosphorylation targets of ATM and involved in the DNA damage checkpoint network (Kurz and Lees-Miller, 2004), it was recently shown that NBS1, MDC1 and 53BP1 also operate upstream of ATM, and that these proteins are recruited at DSB sites within seconds (Bekker-Jensen et al., 2005; Dupre et al., 2006; Lou et al., 2006; Uziel et al., 2003). Thus, it seems that these proteins act both as ATM effectors and as sensors/activators of DNA damage response, taking part in an early cyclic process that amplifies the damage signal by interactions of the sensors with ATM and damaged chromatin (Lavin, 2004; Lou et al., 2006; Shiloh, 2006; Stucki and Jackson, 2006).

1.4.2 Phosphorylation of H2AX and recruitment of repair proteins at DNA DSBs

In close vicinity to a DSB, ATM is the major kinase involved in the phosphorylation of the histone H2AX at Ser139 (Hickson et al., 2004) and the phosphorylated form γ-H2AX can be detected *in situ* as foci shortly after DSB induction (Burma et al., 2001; Fernandez-Capetillo et al., 2004; Rogakou et al., 1998; Stiff et al., 2004). H2AX is a variant of H2A histone and represents up to 25% of the total H2A present within mammalian cells (Rogakou et al., 1998). Phosphorylation of H2AX is involved in the recruitment of chromatin remodeling complexes at DSB lesions (Chai et al., 2005; Flaus et al., 2006). These complexes have been suggested to decondense chromatin and facilitate the access of DNA repair proteins. The importance of the H2AX-dependent chromatin remodeling activities is also implied by the fact that dephosphorylation of γ-H2AX is required for the checkpoint signal switch off (Keogh et al., 2006; Kruhlak et al., 2006b). After DSB induction, γ-H2AX organizes the accumulation of repair-related proteins into nuclear foci and co-localizes with the MRN complex, MDC1, 53BP1, BRCA1 and phosphorylated ATM (pATM) at the DSB-flanking chromatin (Bekker-Jensen et al., 2006; Kobayashi et al., 2002; Paull et al., 2000; Schultz et al., 2000; Stucki et al., 2005). These large aggregates of hundreds to thousands of copies of each protein were proposed to act as anchors that keep the broken DNA ends together during repair (Stucki and Jackson, 2006) and to amplify the DSB signal, ensuring efficient cell cycle arrest during repair (Lou et al., 2006).

1.5 DNA DOUBLE-STRAND BREAK REPAIR

The survival of an organism is highly dependent of its cells ability to efficiently repair the critical DSB lesions. There are two main pathways that repair DSBs in mammalian cells: non-homologous end joining (NHEJ) (*Figure 4A*) and homologous recombination (HR) (*Figure 4B*). Although they are highly conserved in eukaryotes, HR is the major repair process in yeast, while NHEJ predominates in mammalian cells.

During HR, a homologous sequence (usually a sister chromatid) is used as a template to retrieve genetic information from, and to repair the damage. Therefore, HR as a conservative process, is error free. In contrast, NHEJ rejoins the two DNA DSBs directly without the requirement for extensive sequence homology between the DNA ends. Usually, the ends require processing (i.e. removal of a few nucleotides) before ligation, leading to small deletions of DNA sequence. Therefore, NHEJ is considered to be an error-prone repair pathway.

NHEJ was previously shown to act throughout the cell cycle, having a dominant role in G1, whereas HR is restricted to late S/G2, when a sister chromatid is available (Rothkamm et al., 2003). However, the two pathways can compensate and collaborate for efficient DNA double-strand break repair (Delacote et al., 2002; Saintigny et al., 2007). Thus, NHEJ acts as an immediate repair process, while HR proteins continue for a longer time their attempt to repair persistent DSBs (Delacote et al., 2002; Kim et al., 2005). Moreover, NHEJ protein assembly precedes that of HR proteins even in S/G2 phases (Kim et al., 2005). The basic mechanisms of these pathways as well as the proteins involved are outlined below.

1.5.1 NHEJ

The NHEJ repair pathway is mediated by a set of core proteins and processing enzymes (Weterings and van Gent, 2004). The core proteins include the DNA-dependent protein kinase (DNA-PK) and DNA Ligase IV/XRCC4/Cernunnos (also named XRCC4-like factor, XLF) (*Figure 4A*) (Ahnesorg et al., 2006; Buck et al., 2006). DNA-PK consists of a large catalytic subunit, DNA-PKcs, and its regulatory subunits, Ku70 and Ku80. As processing enzymes were suggested Artemis (a nuclease) and DNA polymerases μ and λ (Capp et al., 2006; Ma et al., 2002; Mahajan et al., 2002).

NHEJ repair process is initiated by binding of Ku heterodimer to the ends of broken DNA in a sequence-independent manner, by forming a ring-like structure around DNA ends (*Figure 4A*) (Walker et al., 2001). Thereafter, Ku translocates inwards along DNA and recruits DNA-PKcs (Hammarsten and Chu, 1998; Yoo and Dynan, 1999), which keeps the two ends together, followed by activation of its kinase function (DeFazio et al., 2002) and DNA-PK complex formation. Then DNA-PKcs autophosphorylates on at least seven sites and this is essential for a functional NHEJ (Chan et al., 2002; Reddy et al., 2004). It has been suggested that authophosphorylation leads to conformational changes in DNA-PKcs, that makes the DNA ends reachable for the next step of processing and ligation (Cui et al., 2005; Reddy et al., 2004).

In addition to keeping the two broken DNA ends in a close proximity, a very important role of DNA-PK complex is the recruitment and activation of proteins that

mediate DNA ends processing and ligation. These proteins include Artemis and DNA Ligase IV/XRCC4 complex. The ends are processed if necessary by phosphorylated Artemis which gains endonuclease activity (Goodarzi et al., 2006) and cuts single-strand overhangs (Ma et al., 2002).

The last step, ligation of the DNA ends, is mediated by the DNA Ligase IV/XRCC4/XLF complex (Hentges et al., 2006). The newly identified factor XLF (Cernunnos) associates with the XRCC4/ligase IV complex and amplifies its ligase activity in an unknown manner. XLF was recently shown to be phosphorylated by DNA-PKcs and recruited at DSBs (Wu et al., 2007).

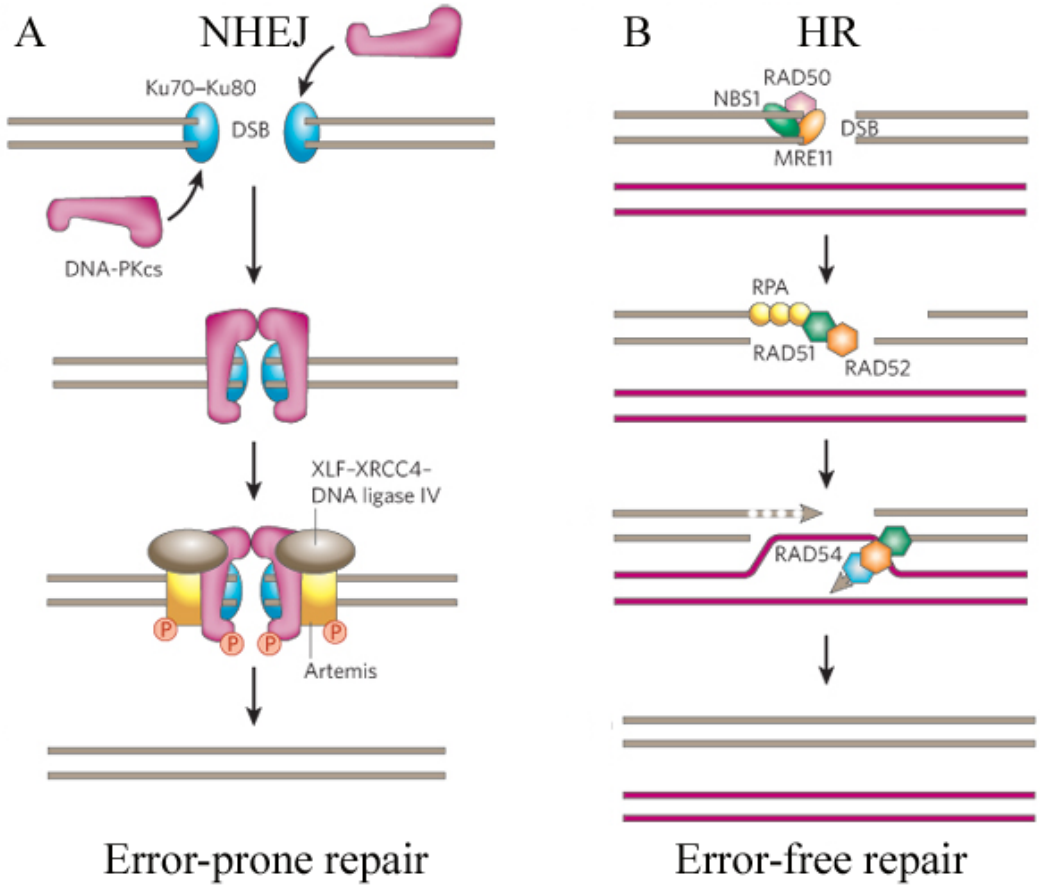

Figure 4. The two major DNA DSBs repair pathways in mammalian cells. (**A**) Non-homologous end joining (NHEJ): Ku heterodimer binds to DNA DSBs and recruits DNA-PKcs. DNA-PKcs autophoshorylates and gain kinase activity. DNA-PK complex phosphorylates and recruits Artemis and DNA Ligase IV/XRCC4/XLF complex to the broken DNA ends. Artemis processes the ends and DNA Ligase IV/XRC4/XLF complex ligates the DNA ends. (**B**) Homologous recombination (HR): MRN complex detects the DSB and resects the DNA ends to form ssDNA overhangs. RPA, RAD51 and RAD52 proteins bind to ssDNA and search for homology in an intact DNA double helix. RAD54 facilitates strand invasion. DNA is synthesized and DNA ends are ligated. Adapted by permission from Macmillan Publishers Ltd: [Nature] (Downs et al., 2007), copyright (2007).

After NHEJ, DNA synthesis may be needed to fill in any remaining gaps, and DNA polymerases are mediating this step. The requirement of XRCC4/ DNA Ligase IV for polymerase and nuclease activity recently led to a proposal of a mechanism for how NHEJ suppresses end processing to preserve the DNA sequence (Budman et al., 2007).

1.5.2 HR

HR plays an important role during S/G2 phase repair in mammalian cells, but also during replication, at stalled replication forks (Lundin et al., 2002).

HR can occur via two different pathways: RAD51-dependent strand invasion and single-strand annealing. HR is initiated by the resection of DNA ends to form 3'-single-stranded DNA (ssDNA) overhangs, and MRN complex is involved in this end-processing (*Figure 4B*) (Adams et al., 2006).

After resection of DNA ends, the 3'-ssDNA overhangs are protected by filaments of replication protein A (RPA), whereas processing of ends is prevented by the binding of RAD52 protein (van Dyck et al., 1999). RAD51 binding to ssDNA is mediated by RAD52, BRCA2 and RAD51 paralogs, and RAD51 replaces RPA. Then the ssDNA-protein filament searches for a homologous region and invades an intact DNA double helix (*Figure 4B*). RAD54 promotes RAD51-mediated DNA strand invasion. It was recently suggested that RAD54-mediated chromatin remodeling coincides with DNA homology search by the RAD51 filament (Kwon et al., 2007). Many aspects of HR pathway, including protein functions and the mechanism of strand invasion are still not completely understood. The last step of HR repair consists of DNA synthesis, disconnection from the template and DNA ends ligation (Krogh and Symington, 2004; Wyman et al., 2004).

2 THE PRESENT STUDY

2.1 AIMS

The present investigation aims to clarify important aspects regarding DNA DSBs induction and repair in human cells exposed to high-LET radiation. The general aim is to understand how high-LET ions interact with DNA and activate the DNA repair pathways.

Specific aims

Specific aims are to determine the importance of chromatin organization for the induction of DNA double-strand breaks, to characterize critical steps in the repair of clustered damage sites and to develop new ways to study DNA repair mechanisms after high-LET radiation exposure.

In particular,

- To analyse the DNA damage induction in human cells irradiated with different radiation qualities (Paper I)
- To determine the relationship between the non-random distribution of DNA DSBs and different types of chromatin organization after irradiation with low- and high-LET radiation (Paper II)
- To quantitate DSBs for different chromatin structures exposed to low- and high-LET radiation (Paper II)
- To study the effects of radiation-induced heat labile sites (HLS) on the analysis of DSB induction and repair in various irradiated mammalian cells (Paper III)
- To investigate the substructure of DNA damage, repair and signalling along high-LET particle tracks (Paper IV)
- To improve qualitative analysis of DBSs in human cells after exposure to high-LET radiation (Paper IV)

2.2 MATERIALS AND METHODS

2.2.1 Cell cultures and inhibitors

In the present studies the following cell lines were used: normal human skin fibroblasts (GM5758), NBS1 defective human fibroblasts (GM7166) or fibroblasts defective in ATM (GM2052D) (Human Genetic Mutant Cell Repository, Camden, NJ, USA); human glioma cells M059J (DNA-PKcs defective) and wild-type M059K (American Type Culture Collection, Manassas, VA, USA); non-small cell lung carcinoma cells U-1810 and erythroblastoid K562 cells; and hamster cell lines AA8 (wild-type) and EM9 (XRCC1 mutant), and mouse fibroblasts A11 (PARP1 mutant). Normal human skin fibroblasts (GM5758) are a stable cell line system, with confluent cells resting in G_0/G_1 and normal DSB rejoining. NBS1 defective human fibroblasts GM7166, human glioblastoma cell line M059K and human lung carcinoma cells U-1810 have been used for their normal DSB rejoining kinetics. The cells were cultured at 37°C, 5% CO2, and were, for the pulsed-field gel electrophoresis experiments, labeled with 1.2 kBq/ml [methyl-^{14}C]thymidine (Amersham, UK) for about two doubling times.

In some experiments, the influence of inhibition of the phosphatidylinositol-3-OH kinase-like kinases (PIKKs) or PARP was examined by using 50μM wortmannin (Sigma-Aldrich) or 5 mM 3-AB (3-aminobenzamide, Sigma-Aldrich), respectively. Cells were incubated with inhibitors before, during and after irradiation.

2.2.2 Description and preparation of the chromatin structures

The different chromatin structures used in Paper II represent a wide range of chromatin compactness, from intact nucleus to naked genomic DNA. Permeabilization of intact cells and removal of soluble proteins lead to condensed chromatin (*Figure 5*). To preserve the chromatin conformation of the intact cells, a physiological concentration of Mg^{2+} and Na^+/K^+ was used. A further relaxation of the condensed chromatin, obtained by using hypotonic ion concentration, produces decondensed chromatin. The condensed and decondensed chromatin are found within the permeabilized nuclei and are attached to the nuclear matrix (Ljungman, 1991; Nygren et al., 1995) (*Figure 5*). Nucleoid chromatin is prepared by removal of all soluble proteins and histones (Ljungman, 1991), leading to a structure consisting of chromatin loops attached to nuclear matrix (*Figure 5*). The naked genomic DNA produced by lysis of the intact cells is almost totally without protein content (Stenerlow et al., 2003).

Agarose plugs containing $2x10^6$ diploid GM5758 cells/ml from confluent cultures were prepared (Hoglund et al., 2000) and treated with four different nuclear preparation buffers, mainly according to Nygren et al. (Nygren et al., 1995) and Oleinick and Chiu (Oleinick and Chiu, 1994). Briefly, a condensed nuclear chromatin organization was obtained by treating plugs for 18 h with an ice-cold solution containing 0.5 % (w/v) Triton X-100, 4 mM Tris, 142 mM KCl, and 0.8 mM $MgCl_2$, pH 7.4. Decondensed nuclear chromatin was attained from condensed chromatin after washing for 3 h in a decondensed solution (0.2 mM EDTA, 8 mM Na_2HPO_4, 1.5 mM KH_2PO_4, pH 7.5) and seven or eight washes (1 h each) in PB^- (8 mM Na_2HPO_4, 1.5

mM KH_2PO_4, pH 7.4). To prepare nucleoid chromatin, agarose plugs containing GM5758 cells were incubated on ice for 18–20 h in a 2 M salt solution [0.5% (w/v) Triton X-100, 4 mM Tris, 1.85 M NaCl, 0.15 M KCl, 5 mM $MgCl_2$, pH 7.5]. ‘‘Naked’’ genomic DNA was prepared by treating the cells for 18 h with a lysis buffer containing 2% (w/v) sarcosyl, 1 mg/ml Proteinase K (Boehringer-Mannheim, Germany) in 0.5 M EDTA, pH 8.0; the samples were incubated on ice for 1 h and were then put at 50°C under gentle shaking. To ensure complete removal of EDTA, proteins and cell debris from the agarose plugs, samples for condensed, nucleoid and DNA structures were washed seven or eight times (≥1 h each) in PB^+ (8 mM Na_2HPO_4, 1.5 mM KH_2PO_4, 133 mM KCl, 0.8 mM $MgCl_2$, pH 7.4). Intact cells and naked DNA from K562 cells in agarose plugs (containing 5 x 10^6 cells/ml) were prepared as above. The agarose plugs were irradiated in serum-free medium (for intact cells), in PB^+ (condensed, nucleoid and DNA structure), or in PB^- (decondensed chromatin). The agarose plugs containing naked DNA from K562 cells were irradiated in the presence of a scavenger (200 mM Tris-HCl and 2 mM EDTA, pH 7.5).

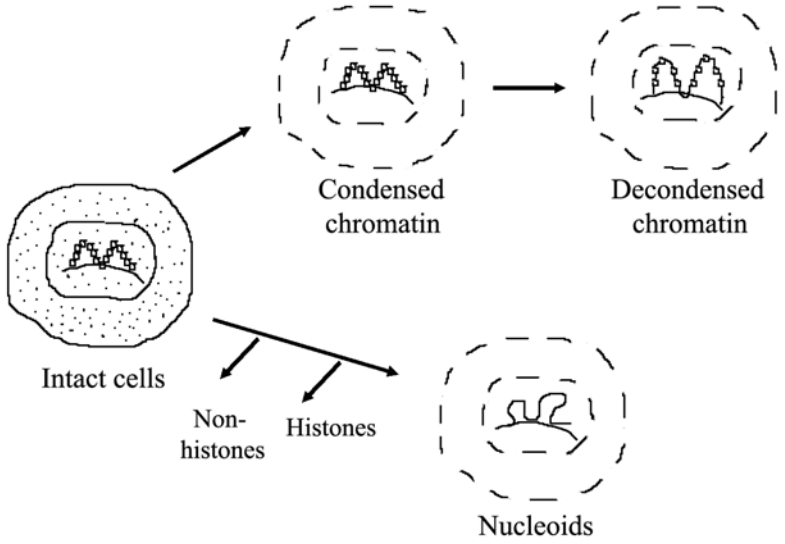

Figure 5. Schematic representation of different chromatin structures preparation. See text for details. Adapted and modified from (Ljungman, 1990).

2.2.3 Irradiation

Cells grown in dishes were irradiated with low-LET ^{60}Co (Paper IV) or ^{137}Cs photons (Gammacell 40 Exactor MDS Nordion, Canada; 1.3 Gy/min dose rate), or with high-LET radiation (80 - 320 eV/nm nitrogen ions, 40-160 eV/nm boron ions and 225-300 eV/nm neon ions) at The Svedberg Laboratory, Uppsala University, as previously described (Stenerlow et al., 2000). To avoid initiation of repair and signaling processes, cells were placed on ice prior and during irradiation.

For the foci analysis, cells cultured on microscope slides were irradiated with 80 – 320 eV/nm high-LET nitrogen ions under a low angle (< 5°) between the ion beam direction and the cell monolayer plane (*Figure 6*).

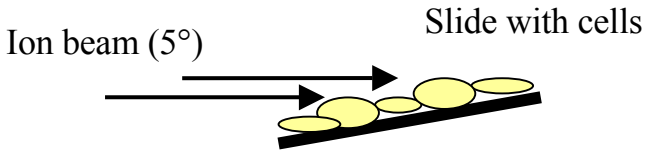

Figure 6. Low angle irradiation

The average nuclear area of a flat confluent fibroblast (GM5758) was 230 μm^2 on a horizontal projection (Karlsson and Stenerlow, 2004), with a mean diameter of the nucleus of 17.1 μm and a mean nuclear thickness of 2 μm. For irradiation under an angle of 5º, the elliptical area of the mean cross section of (17.1 μm/2 x [2 μm/2 + (17.1 μm x sin 5º)/2] x π) = 47 μm^2 was calculated, as described by Jakob et al. (Jakob et al., 2003). The irradiation doses (0.56 – 2.25 Gy) were chosen to give an average of 2 particle tracks/ nucleus, and calculated by using

$$N = \frac{1}{0.1602} \cdot \frac{D \cdot A}{LET}$$

where N is the number of hits per nucleus, D dose in Gy, A cross sectional area of the nucleus in μm^2 and LET is the LET in keV/μm. The term $1/0.1602$ comes from the conversion from J to eV ($1eV = 1.6 \times 10^{-19} J$). The number of tracks per nucleus follows a Poisson distribution with an average of 2 particle traversals/ nucleus. The irradiation parameters are stated in *Table 1*.

Table 1. Irradiation with nitrogen ions under 5º angle.

LET (eV/nm)	Energy (MeV/nucleon)	Dose (Gy)[a]
80	36.0	0.6
160	15.4	1.1
320	6.1	2.2

[a] Assuming a mean of two particle traversals per nucleus for irradiation under an angle of 5º.

2.2.4 Pulsed-field gel electrophoresis (PFGE) and DSB analysis

After irradiation, cells were allowed to repair for 0 – 20 h and then were embedded in agarose plugs. The cells were lysed for 24 h in ice cold lysis buffer (2 % (w/v) sarcosyl, 1 mg/ml Proteinase K (Roche Diagnostics, Mannheim, Germany) in 0.5 M EDTA, pH 8.0), followed by ≥10 h treatment with ice cold 2 M salt solution (1.85 M NaCl, 0.15 M KCl, 5 mM $MgCl_2$, 2 mM EDTA, 4 mM Tris, 0.5% Triton X-100, pH 7.5), in order to ensure the DNA extraction without induction of additional DSB originating from heat-labile sites (Stenerlow et al., 2003) (*Figure 7*). The warm lysis protocol, consisting of cell lysis overnight at 50°C (2 % sarcosyl, 1 mg/ml Proteinase K in 0.5 M EDTA, pH 8.0) was also used in Paper I and Paper III.

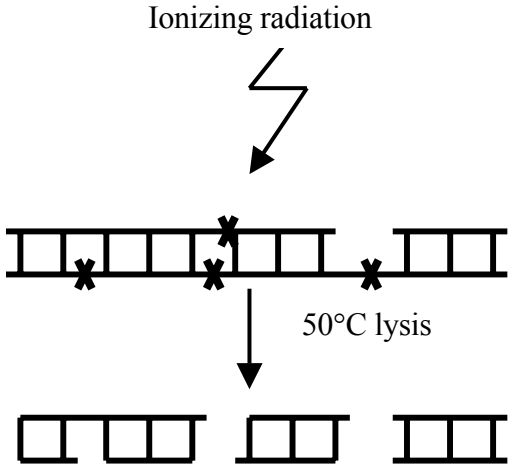

Figure 7. Proposed model for conversion of heat-labile sites (**X**) into DSBs, as a result of post-irradiation heat exposure during conventional lysis. Two HLS or a SSB and a HLS located closely but on opposite DNA strands, could be revealed as a DSB during the warm lysis protocol used in the standard PFGE assay.

The DNA fragments within the agarose plugs were separated in the size range 5 kbp - 6 Mbp by running two different PFGE protocols, and the fraction of [^{14}C] –DNA radioactivity released was analyzed by liquid scintillation for each gel segment, as previously described (Hoglund and Stenerlow, 2001). For correct determination of DSB after high-LET irradiation, the number of DNA fragments (n) in each size range (*Table 2*) can be calculated by:

$$n\left(M_i\right) \cong \frac{F_i}{M_i} \qquad \textit{DNA fragmentation analysis}$$

where F_i is the fraction of DNA in a gel segment with the mean fragment size M_i within that segment. The total number of DSBs induced is assessed by adding the yields for every size interval. After more than 10 h repair, the DNA-fragment distribution in high-

LET irradiated cells becomes close to random (Stenerlow et al., 2000), and calculation of the remaining DSBs after 20 h of repair was therefore based on the fraction of DNA <5.7 Mbp, assuming random distribution of DSBs (Blocher, 1990; Stenerlow and Hoglund, 2002). Thus, the number of randomly induced DSBs is related to the fraction of activity released (FAR) in a non-linear manner:

$$F_{<k} = 1 - e^{-\frac{rk}{n}\left(1 + \frac{rk}{n}\left(1 - \frac{k}{n}\right)\right)} \qquad \textit{FAR conventional assay}$$

where $F_{<k}$ is the fraction of DNA with sizes smaller than the threshold size k (5.7 x 10^6 bp), r is the number of DSBs per chromosome, and n is the mean size of a chromosome (130.4 x 10^6 bp).

Table 2. Gel segments

DNA size interval (kbp)	Mean size, M_i (kbp)	Width, δM_i (kbp)
3500-5700	4600	2200
1110-3500[a]	2305	2390
930-1110	1020	180
680-930	805	250
375-680	527	305
225-375	300	150
145-225	185	80
97-145	121	48
48-97	73	48
0-48	24	48

[a]The segment originates from two different PFGE gels, optimized to separate DNA fragments of different sizes. The fraction of DNA <1110 kbp in the 5-1500 kbp gel was subtracted from the fraction of DNA <3500 kbp in the 1-6 Mbp gel.

2.2.5 Immunofluorescence detection and analysis of foci

After indicated repair times, cells grown on microscope slides were washed in serum free medium and fixed for 20 min in methanol (- 20°C), followed by permeabilization in ice-cold acetone for 10 s. After washing and blocking in 10% FCS-PBS for 1 h at room temperature, cells were incubated for 1 h at 37°C with the following primary antibodies (dilution 1:250 – 1:1000 in 1% FCS-PBS): anti-phospho-H2AX (Ser139) (mouse; Upstate Biotechnology, Lake Placid, NY), anti-phospho-ATM (Ser 1981) (rabbit; Rockland Immunochemicals for Research, Gilbertsville, PA), anti-MRE11 (rabbit; Oncogene Research Products, San Diego, CA), and anti-53BP1 (rabbit; Bethyl Laboratories, Montgomery, TX). After washing in PBS, the cells were incubated for 1 h at 37°C with secondary antibodies Alexa Flour 488 and Texas Red or Alexa Flour 555 (Molecular Probes, Eugene, OR) (dilution 1:400). Nuclei were counterstained with DAPI (0.1 µg/ml) for 1 min at room temperature, followed by 10 min air dry, and the

slides were mounted in Vectashield antifade solution (Vector Laboratories, Burlingame, CA).

Images of cells were captured with a CCD camera on a Zeiss LSM 510 META confocal microscope using a 100x objective, and processed using Adobe Photoshop 6.0. From each slide, images containing about 40 nuclei were recorded at a 0.3 μm interval, as sets of optical sections across the thickness of the cells. For computer analysis of foci, images were acquired as 24-bit RGB images using a Spot Insight Colour CCD camera (Diagnostic Instruments, Sterling Heights, MI) coupled to a Nikon Eclipse E400 fluorescence microscope with a Plan Flour 40x objective (Nikon Corporation, Tokyo, Japan). All digital image analysis methods have been implemented in Java as plug-ins to the digital image analysis software ImageJ (Abramoff et al., 2004). The image analysis process of the γ-H2AX images was based on a Gaussian filter followed by an edge detecting Laplace filter and thresholding, which extracts the foci from the background (Qvarnstrom et al., 2004; Sonka et al., 1998). The processed foci images were merged with threshold images of the nuclear stainings resulting in images with defined regions of foci, nuclear area and background. These images were used as templates to measure inter foci distances. Tracks with four or more foci (50 - 177 tracks per data point) were included in the analysis, and number of foci and total track length was recorded for each track using a plug-in to ImageJ that labels and counts the foci.

2.3 SUMMARY OF THE PAPERS

2.3.1 Paper I

Radiation quality dependence of DNA damage induction

Analysis of DNA fragmentation and repair in relation to radiation quality may give important information about the role of break complexity and correlated DSBs.

In this study we used pulsed-field gel electrophoresis (PFGE) to analyse the DNA fragment distribution after exposure to radiation of different ionisation densities. Normal human fibroblasts were irradiated with boron ions (40-160 keV/μm), nitrogen ions (80-225 keV/μm) and neon ions (225-300 keV/μm). We reported that the amount of DNA less than 1.1 Mbp decreased with increasing LET for all three ions.

In conclusion, high-LET nitrogen ions were shown to produce an excess of DNA fragments up to 1-3 Mbp. This non-random distribution of fragments, probably produced by intra-track correlated DSBs, may constitute a significant fraction of the total number of DSBs.

2.3.2 Paper II

Chromatin organization contributes to non-randomly distributed double-strand breaks after exposure to high-LET radiation

Little is known about the cause of the non-random fragmentation of DNA, but it has been suggested that both higher-order chromatin organization and the track structure of high-LET radiation are important.

In this study, the influence of higher-order chromatin structure on the non-random distribution of DNA DSBs induced by high-LET radiation was investigated. Five different chromatin structures (intact cells, condensed and decondensed chromatin, nucleoids and naked genomic DNA) from GM5758 fibroblasts or K562 tumor cells were irradiated with ^{137}Cs γ-ray photons and 125 keV/μm nitrogen ions. DNA was purified with a modified lysis procedure to avoid release of heat-labile sites, and fragment size distributions and DSB yields were analysed by PFGE. We found that while DSBs in photon-irradiated cells were randomly distributed, irradiation of intact K562 cells with high-LET nitrogen ions produced an excess of non-randomly distributed DNA fragments 10 kb–1 Mbp in size. Moreover, complete removal of proteins eliminated this non-random component. There was a gradual increase in the yield of DSBs for each chromatin decondensation step. The corresponding relative biological effectiveness (RBE) decreased from 1.6–1.8 for intact cells to 0.49 for the naked DNA.

In conclusion, we found that DNA organization into chromatin fiber and higher-order chromatin structures is responsible for most of non-random distributed DSBs induced by high-LET radiation. In addition, DSB yields calculated by fragmentation analysis and RBE values were strongly influenced by chromatin compactness. However, our data suggest a complex interaction between track structure and chromatin organization over several levels.

2.3.3 Paper III

Repair of radiation-induced heat-labile sites is independent of DNA-PKcs, XRCC1 or PARP

When several non-DSB lesions are clustered within a short distance along DNA, or close to a DSB, they may interfere with the repair of DSBs and affect the measurement of DSB induction and repair. It was recently shown that a large fraction of DSBs measured by PFGE is due to radiation-induced heat-labile sites (HLS) within clustered lesions, as a result of an artifact that occurs during preparation of genomic DNA at elevated temperatures.

The newly developed cold lysis protocol was used to accurately measure the number of DSBs. To further characterize the influence of HLS on DSB induction and repair, four human cell lines (GM5758, GM7166, M059K, U-1810) with apparently normal DSB rejoining were tested for bi-phasic rejoining after gamma irradiation. Removal of artifactual DSBs decreased the fraction of fast rejoining to less than 50%. At t=0 the HLS accounted for more than 40% of the DSBs, corresponding to 10 extra DSB/cell/Gy in the initial DSB yield. These heat-released DSBs were rejoined within 60-90 min in all tested cells, including M059K cells treated with wortmannin or DNA-PKcs defect M059J cells. Furthermore, cells lacking XRCC1 or Poly(ADP-

ribose) polymerase-1 (PARP-1) rejoined both total DSBs and heat-released DSBs similar to normal cells.

In summary, the presence of HLS has a substantial impact on DSB induction yields and DSB rejoining rates measured by PFGE. Our data suggest that the lesions involved in the release of HLS into DSBs are repaired independent of DNA-PKcs, XRCC1 or PARP-1, and that human cells without functional DNA-PK activity have no fast rejoining of DSBs.

2.3.4 Paper IV

ATM phosphorylation and formation of repair protein foci at clustered DNA damage sites

In connection to the use of high-LET radiation in tumor therapy, there is a strong need for more knowledge on the cellular processes involved in the repair of clustered DNA lesions induced by such radiation.

In this study we monitored, by immunofluorescence, the spatial dynamics of DNA damage signalling proteins in human fibroblast cells exposed to high-LET ions. Foci of γ-H2AX, 53BP1 and MRE11 rapidly co-localized and formed tracks of ion trajectories through the cell nucleus. Track morphology varied with LET and repair time. However, the mean distance between two adjacent γ-H2AX foci was constant irrespective of LET (80-320 eV/nm) and repair time (5-240 min). This was in strong contrast to the number of DSBs present on each track, indicating that a single γ-H2AX focus may contain clusters of several DSBs within 1-2 Mbp of chromatin. Interestingly, high-LET ion track irradiation revealed one of the earliest responses to ionising radiation, ATM phosphorylation (Ser1981), as pATM foci that clearly correlated with γ-H2AX foci within ion tracks, as well as punctuated/diffuse staining dispersed throughout the whole nucleoplasm (5-240 min post-irradiation). Thus, we suggest that most of ATM phosphorylation might be associated with chromatin changes or other signalling processes that take place at distance from DSBs.

In conclusion, our data provide new insights on the spatial dynamics of DNA damage signalling and repair on a subnuclear level along high-LET ion tracks.

2.4 DISCUSSION AND CONCLUSIONS

Radiation therapy is used in attempting to kill tumor cells by producing DNA double-strand breaks. To efficiently treat malignant tumors that are deeply seated, current tumor therapy uses high-LET radiation, such as accelerated ions or radioactive nuclides emitting α-particles. Radiation of various LETs differ in their biological effectiveness. However, the molecular mechanisms linking DSB incidence to cell death are still unknown. Therefore, studies of DSB induction and repair in relation to radiation quality could help identifying critical steps of this process and be of great importance for improvement of tumor therapy. DSB is probably a very heterogeneous type of damage and several factors might influence their recognition and reparability, including the amount of DSBs, the distribution within chromatin and the complexity (*i.e.* the presence of additional DSBs or other DNA lesions in close vicinity). In the present investigation we studied several aspects of DNA DSBs induction and repair after exposure to ionising radiation of different qualities, including the role of DNA damage clustering and chromatin organization, as well as the activation of repair-associated proteins at clustered DNA damage sites in human cells.

2.4.1 High-LET radiation induce a significant non-random distribution of DNA fragments

Analysis of DNA fragmentation after exposure to high-LET radiation can bring information on break complexity and clustered DSBs. DNA fragment distribution in human fibroblasts after exposure to different radiation qualities has been analysed by using pulsed-field gel electrophoresis. We reported that the amount of DNA less than 1.1 Mbp decreased with increasing LET for all ions used. The normalized fraction of DNA versus fragment size showed that, after high-LET radiation, DSBs were non-randomly distributed, with an excess of fragments up to 1-3 Mbp in size (*Figure 8*) (Paper I). This was not found after exposure to low-LET photons, when the breaks are following a random Poisson distribution (Hoglund and Stenerlow, 2001; Newman et al., 1997). The excess of small fragments represents half of the total number of DSB that is measured by fragmentation analysis (Hoglund et al., 2000). Thus, high-LET radiation induces a significant non-random distribution of DNA fragments, probably due to intra-track correlated DSBs. To extrapolate to a single particle traversal, it was calculated that a single particle traversal could produce several DNA fragments less than 1Mbp in size.

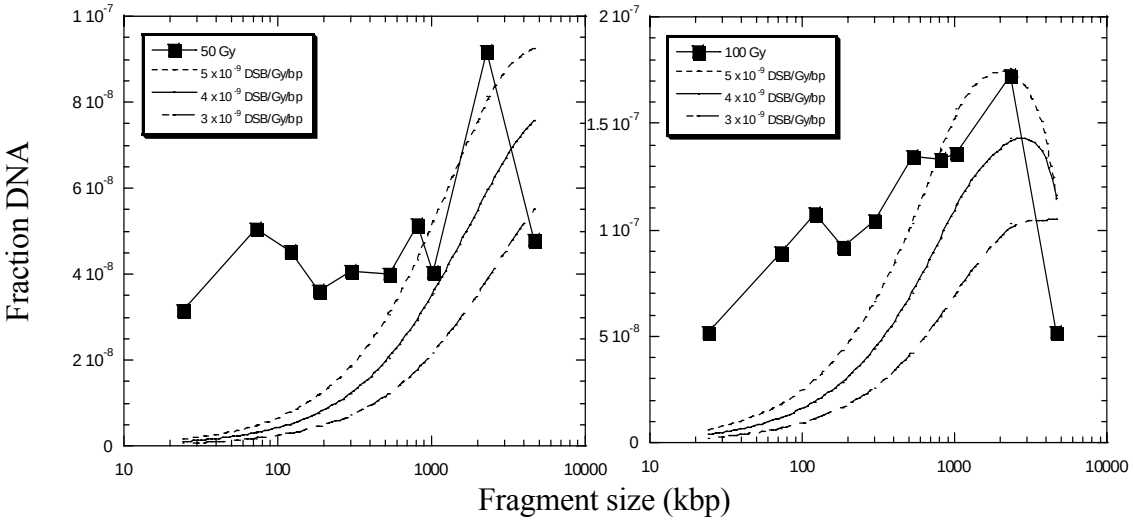

Figure 8. Fraction of DNA, normalized for the molecular weights within the different gel segments, versus fragment size in normal human fibroblasts irradiated with nitrogen ions of 225 eV/nm. The curves without data points represent random theoretical distribution of the breaks, according to Blocher's model (see section 2.2.4).

2.4.2 Chromatin organization is responsible for non-random distribution of DSB after high-LET radiation

The non-random distribution of DSBs after high-LET radiation was suggested to be linked to the chromatin organization into loops, and also to the particle track structure (Hoglund and Stenerlow, 2001; Rydberg, 1996; Rydberg, 2001), but direct evidence to support this hypothesis has not been presented. By modifying the chromatin structure, we found that DNA organization into chromatin fiber and higher-order chromatin structures is responsible for most of non-random distributed DSBs induced by high-LET radiation (Paper II). This was clearly seen when irradiating intact K562 cells or naked genomic DNA from K562 cells under high-scavenging conditions (200 mM Tris-HCl and 2 mM EDTA), to study only the direct effect of radiation (*Figure 9*). After high-LET ion irradiation, the difference in DSBs distributions for small fragments (10 kbp – 1 Mbp) was only due to chromatin organization (*Figure 9B*). In contrast, the DSB distributions for intact cells and naked DNA after photon irradiation were both close to random (*Figure 9A*). Assuming that the high-LET induced DNA fragmentation consists of one random and one non-random component (Hoglund and Stenerlow, 2001), the non-random component alone can give information on the intratrack ion interaction with chromatin. However, complex interactions between the particle track and different levels of chromatin organization may require simulation using several probability functions to approximate the experimental data.

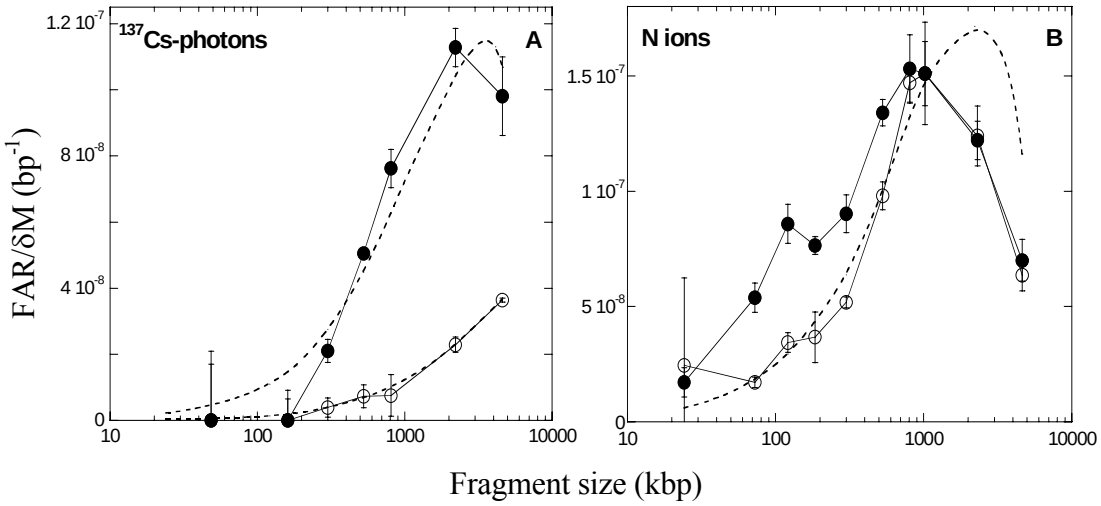

Figure 9. The normalized fraction of DNA, as a function of DNA fragment size, for intact K-562 cells irradiated with 80 Gy (•) and naked DNA irradiated with 40 Gy in the presence of 200 mM Tris and 2 mM EDTA (o). The dotted curves represent random theoretical distribution of the breaks, according to Blocher's model (see section 2.2.4).

To investigate in greater detail the influence of higher-order chromatin organization on DNA fragment distributions, we used five different chromatin structures from GM5758 human fibroblast cells: intact cells, condensed chromatin, decondensed chromatin, nucleoids and naked genomic DNA without any proteins. The DSB distribution was clearly non-random for intact cells irradiated with nitrogen ions, while for all the other chromatin structures they approached the random theoretical curves for fragments smaller than 1 Mbp. The strong deficiency of fragments larger than 1 Mbp (as in *Figure 9B*) might be due to the fact that there is a low probability that high-LET nitrogen ions would produce sparsely located breaks which lead to Mbp-sized fragments. A particle track will most probably intercept the chromatin fiber in the close vicinity of a previous hit, producing smaller size DNA fragments. Since the irradiation was performed under low scavenging conditions, the high-energy δ electrons (ejected from atoms by the passage of nitrogen ions) may produce a significant fraction of low-LET radiation, which may mask a potential non-random component in condensed and decondensed chromatin. In accordance, it was found that DSB distribution for cell monolayers and nuclear monolayers with condensed or decondensed chromatin from Chinese hamster V79 cells after exposure to α particles, were non-random for fragments of 10 – 300 kbp in size (Newman et al., 2000). Our data also suggest clustering of breaks within chromatin loops of 10 kbp – 1 Mbp in size, after nitrogen ion irradiation. The chromatin loop sizes are not exactly known, but several studies have indicated that they are in the range of 10 – 200 kbp (Filipski et al., 1990; Jackson et al., 1990), while fluorescence *in situ* hybridization (FISH) studies on G_0/G_1-phase human cells found loops in the Mbp range (Sachs et al., 1995). Moreover, it was shown that the non-randomly distributed breaks could contribute to fast rejoining (Stenerlow et al., 2000), which could be explained by rapid misrejoining of breaks found in a close vicinity (Kuhne et al., 2000).

2.4.3 DSB yields and RBE values vary strongly when the chromatin structure becomes more open and the proteins are extracted

It was recently shown that a large fraction of DSBs measured by PFGE is due to radiation-induced heat-labile sites (HLS) within clustered lesions, as a result of an artifact that occurs during preparation of genomic DNA at elevated temperatures (Stenerlow et al., 2003). The newly developed cold lysis protocol was used to accurately measure the number of DSBs, which can, otherwise, be overestimated by 35-40% in intact cells irradiated with low-LET photons (Stenerlow et al., 2003). In addition, a detailed analysis of smaller fragments lead to a precise determination of DSBs, their number increasing with about 100% (Hoglund et al., 2000). Extraction of nuclear proteins and a more open chromatin structure leads to increased DSB yield for each decondensation step (*Table 3*). Compared to intact cells, the yields for naked DNA (in buffer without scavengers) increased 83 and 25 times after photon and nitrogen-ion irradiation, respectively. This increase mainly depends on the relative contribution of direct and indirect effects of radiation. Thus, in terms of DSB yields, the removal of nuclear proteins was more effective for photon irradiation than for high-LET radiation (*Table 3*), in accordance to the data by Newman et al. (Newman et al., 2000).

Table 3. DNA DSB yields after γ and N ion irradiation of different chromatin structures from GM5758 cells

Chromatin structure	DSB/cell/Gy[a]		RBE
	γ radiation	N ions irradiation	
Intact cells	27	44	1.6
Condensed chromatin	156	66	0.42
Decondensed chromatin	498	126	0.25
Nucleoids	2526	1062	0.42
Naked DNA	2238	1128	0.49

[a]Assuming that the cell is diploid and contains $6x10^9$ bp

2.4.4 Heat-labile sites (HLS) affect the fast component of DSB rejoining

In addition to the substantial impact on DSB induction yields, the presence of HLS influences also the DSB rejoining rates measured by PFGE. In agreement with previous data (Stenerlow et al., 2003), it was found that the conversion of HLS into DSB during the warm lysis led to an increase of the initial DSB yield by 10 DSBs/cell/Gy, when four different human cell lines were exposed to gamma radiation

(*Figure 10*) (Paper III). A similar contribution of HLS to the total DSB yield was observed in human M059K cells treated with wortmannin, in M059J cells (DNA-PKcs-/-), and three rodent cell lines. About 27 prompt DSBs/cell/Gy (no artifactual release of HLS into DSBs) are induced in human diploid cells (Paper II-III), which is in line with previous studies reporting 23-27 γ-H2AX foci/cell/Gy (Leatherbarrow et al., 2006; MacPhail et al., 2003; Rothkamm et al., 2003; Schultz et al., 2000). Moreover, the presence of HLS generating additional DSBs influences also the bi-phasic DSB rejoining. In particular, the fraction of DSBs rejoined by the fast phase decreased for the cold lysis protocol, while the fast and slow rejoining half-times were similar for both lysis protocols.

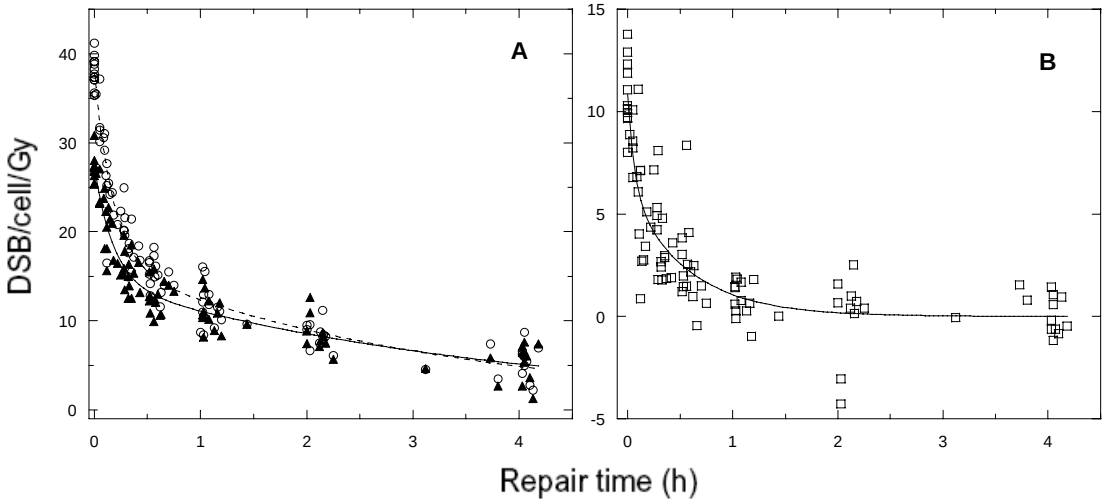

Figure 10. Rejoining of DSBs in GM5758, GM7166, M059K and U-1810 human cells after exposure to 40 Gy gamma radiation. (A) Cells were lysed using standard warm protocol at 50°C measuring total DSBs (○), or a cold protocol at 4°C measuring prompt DSBs (▲). (B) Rejoining of HLS that are released as DSBs in standard PFGE assay. Data points represent the difference between the DSB number obtained by standard warm protocol and by the cold protocol, in A.

2.4.5 Heat-released DSBs are repaired independent of DNA-PKcs, XRCC1 or PARP-1

In addition, cells lacking functional DNA-PKcs did not show any fast DSB rejoining. The only fast rejoining seen in these cells was due to HLS repair, which is monitored using conventional lysis. This might explain previous data on fast rejoining in NHEJ mutants (Chen et al., 1996; Dahm-Daphi et al., 1993; DiBiase et al., 2000; Wang et al., 2001). Our results are similar to recent data on DNA-PK deficient cells (Gulston et al., 2004; Stenerlow et al., 2003), and suggest that the repair of heat-released DSBs is through a non-DSB repair mechanism, which does not involve DNA-PK.

It was proposed that radiation-induced HLS are sugar damages caused by hydroxyl radicals and they can be converted to SSB after alkaline or heat treatment

(Rydberg, 2000) (*Figure 7*). As a result, two HLS or a SSB and a HLS located closely, but on opposite DNA strands, could be revealed as a DSB during the warm lysis protocol used in the standard PFGE assay. Therefore, heat-induced DSBs persistence would be related with both HLS repair and with SSB repair (when a SSB is opposed to an HLS). It is possible that the repair of HLS involves the repair mechanism for sugar damages, which is not well known at the moment. The removal of potential heat-released DSB was fast in eight tested cell lines, with no heat-released DSBs unrejoined after 1-1.5 h post-irradiation (*Figure 10*). The fast kinetics had a half time of 2-3 min, which is in the range of 2-14 min reported for SSB repair (Dahm-Daphi et al., 2000; Potter et al., 2002). It was shown that PARP-1 (poly(ADP-ribose) polymerase-1) and the nuclear scaffold protein XRCC1 play important roles in the SSB repair process (Caldecott, 2003). However, both EM9 (deficient in XRCC1) and A11 (deficient in PARP-1) cells removed potential heat-released DSBs at similar rates as wild type AA8 cells. Thus, the lesions involved in the release of HLS into DSB are repaired independent of XRCC1 or PARP-1, through a non-SSB repair process.

2.4.6 ATM phosphorylation is independent of the localization and level of DNA damage

In relation to the use of high-LET radiation in tumor therapy, there is a strong need for more knowledge on the cellular processes involved in the repair of clustered DNA lesions induced by such radiation. The substructure and spatial dynamics of DNA damage signaling proteins were monitored by immunofluorescence in human fibroblasts cells exposed to high-LET ions (Paper IV). By using low angle high-LET irradiation, we found that phosphorylated ATM, one of the earliest responses to ionizing radiation, accumulated into few pATM foci that clearly correlated with the ion track, and also a punctuated and/or diffuse random staining throughout the nucleoplasm (*Figure 11*). This is in agreement with previous findings suggesting that chromatin alterations might trigger ATM activation even at distance from the DSB site (Bakkenist and Kastan, 2003). Recently, Kruhlak et al. (Kruhlak et al., 2006a) found that pATM initially accumulated at the DSB sites concomitantly with local chromatin decondensation, while at 5 min after laser microirradiation, pATM started to migrate from DSB to the neighboring nucleoplasm. In line with previous findings (Bakkenist and Kastan, 2003), we observed a diffuse pATM staining pattern at 5 min after high-LET ion irradiation, and it is possible that observations at earlier time points could add important information on ATM phosphorylation in response to high-LET irradiation. The presence of pATM far away from the DSB sites from 5 – 240 min brings up several important questions: 1) what initiates/mediates the ATM relocalization and phosphorylation, 2) what is the role of ATM at these sites, and 3) is the nucleoplasmatic pATM bound to chromatin? It also remains unclear if the chromatin relaxation is local (at the DSB sites) or if it is spread throughout the whole nucleus. The early local and ATM-independent chromatin relaxation at DSB sites (Kruhlak et al., 2006a) was suggested to be followed by a wave of chromatin decondensation (ATM-dependent) that is sensed throughout the whole genome (Ziv et al., 2006). Furthermore, the checkpoint protein CHK1 is rapidly phosphorylated by ATM/ATR at sites of DSB

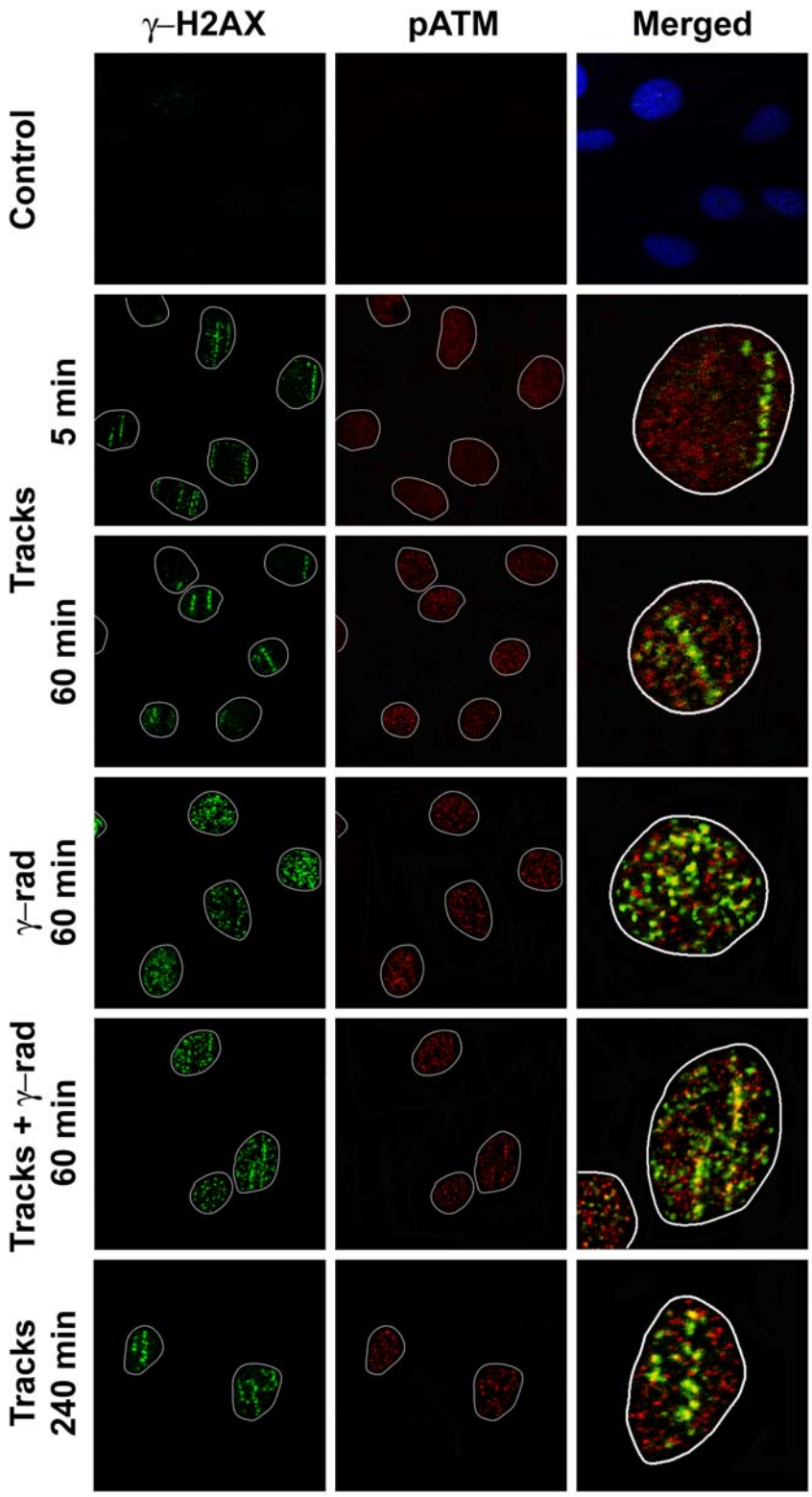

Figure 11. Partial co-localization of pATM and γ-H2AX foci in human GM5758 cells exposed to high-LET ion tracks. Cells unexposed or exposed to nitrogen ions under a low angle were fixed 5 min, 60 min or 240 min post-irradiation. A 10 Gy ^{60}Co-photon irradiation was used as single irradiation or in addition to the low angle nitrogen ions irradiation, and cells were fixed after 60 min. Cells were immunostained against γ-H2AX (green) and pATM (red). Magnification was x1000 for enlarged images and x200 for the rest.

and dissociates from chromatin (Smits et al., 2006). Aside from chromatin relaxation as a possible requirement for correct repair, it is possible that pATM presence at a distance from DSB sites might have a role in cell cycle checkpoint activation. Moreover, the pATM staining pattern showed high similarity for doses between 1-11 Gy of nitrogen ions and/or photons (*Figure 11*), strongly suggesting that most of the ATM phosphorylation after irradiation is not related to the number of DSBs, and is not dependent on the radiation quality. This observation supports the finding that the whole cellular content of ATM can be activated by very few breaks in the DNA (Bakkenist and Kastan, 2003).

In response to DSB induction, ATM activates both cell cycle arrest and an end-processing pathway involved in DNA repair (Riballo et al., 2004). The ATM-Artemis-dependent end-processing pathway, which includes NBS1, MRE11, 53BP1 and H2AX, is proposed to act prior to NHEJ ligation, especially on a subset of highly complex DSBs that are rejoined with slow kinetics (Riballo et al., 2004). Thus, the track-related pATM foci that we found in high-LET irradiated cells may represent complex DSBs that require ATM-Artemis-dependent pathway, and are slowly rejoined, gaining advantage of the ATM-dependent cell cycle arrest (Jeggo and Lobrich, 2006; Riballo et al., 2004). Furthermore, HR may also be involved in the repair of clustered damages, since this pathway was reported to be more active after high-LET radiation, compared to photon radiation (Olsson et al., 2004).

2.4.7 Single foci of γ-H2AX, MRE11 and 53BP1 may represent clusters of DSBs

High-LET radiation induce DSBs that are mainly localized in the center of the track, along the ion trajectory, in contrast to the random nuclear distribution of DSBs observed for γ-radiation (Paper II). At early time points, the mean distance between two adjacent γ-H2AX foci was constant irrespective of the number of induced DSBs (3.5 times more breaks per track unit for 320 eV/nm compared to 80 eV/nm, as measured by PFGE) (*Table 4*). This implicates that each focus represents multiple DSBs for the higher LET (160 - 320 eV/nm) and supports previous observations of

Table 4. Mean distance between γ-H2AX adjacent foci and the number of DSBs per ion track, shortly after irradiation with nitrogen ions of different LET

LET (eV/nm)	Mean distance between foci (μm)	DSB/cell/track unit[a]	Protein focus: DSB
80	1.7 ± 0.4	6.5	1:1
160	1.6 ± 0.3	14.7	1:2.5
320	1.6 ± 0.3	21.2	1:3.5

[a] One track unit is 10μm in length.

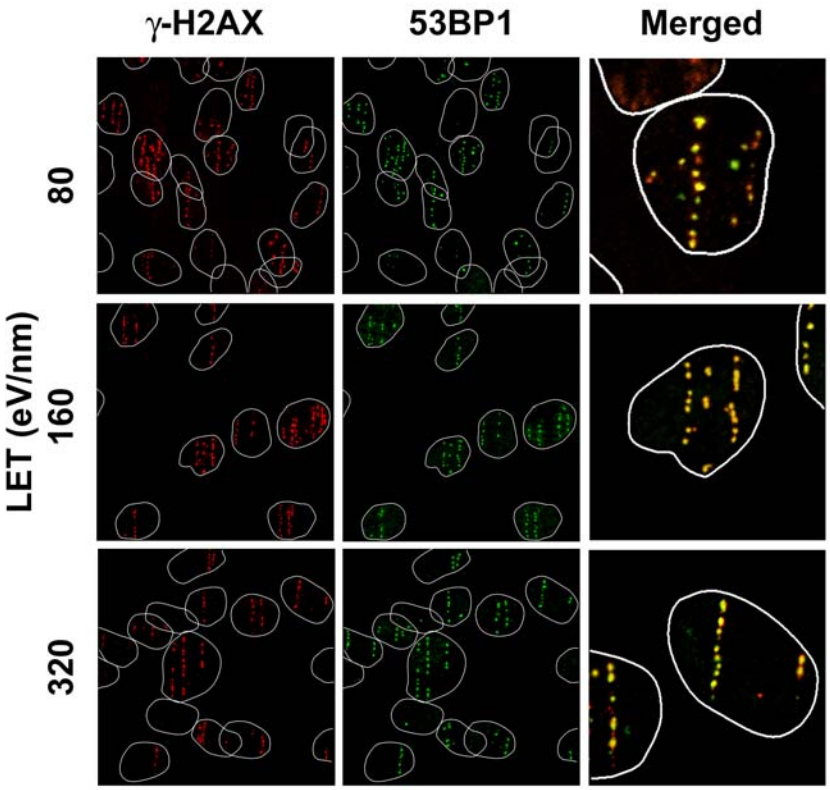

Figure 12. Nuclear distribution of γ-H2AX and 53BP1 foci in GM5758 cells irradiated with nitrogen ions of different LETs (80-320 eV/nm), under a low angle. Cells were exposed to an average of two high-LET ion tracks/cell, fixed 5 min after irradiation, and immunostained against γ-H2AX (red) and 53BP1 (green). Magnification was x1000 for enlarged images and x200 for the rest.

similar foci patterns for a wide range of LETs (Jakob et al., 2003). Moreover, the initial phosphorylation of H2AX protein may not be correlated with the number of DSBs, since multiple DSBs within 1-2 Mbp may saturate the phosphorylation of H2AX (Rogakou et al., 1998). MRE11, 53BP1 and γ-H2AX protein foci co-localized along high-LET ion tracks, indicating the presence of these proteins at identical DSB clusters (*Figure 12*). A similar foci pattern, characterized as protein assembly at the DSB-flanking chromatin, was also seen at 1 h after microlaser irradiation (Bekker-Jensen et al., 2006). Although the functional significance of protein assembly into large foci at DSBs is not fully understood, chromatin modification appears to be a key event in recruiting/activating DNA damage response proteins at DSB sites. These chromatin modifications most likely involve relaxation and disruption of nucleosome stacking (Huyen et al., 2004). Considering the clustering of DSBs after high-LET irradiation, it is possible that such modified regions of chromatin will overlap and this may greatly influence the repair/misrepair of clustered DSBs. At 20 h post irradiation, about 60% of the cells showed 1-5 large and co-localized γ-H2AX, 53BP1 and MRE11 foci per nucleus, that most likely represent complex breaks that are still unrepaired. This assumption is supported by the fact that a higher LET resulted in

more DSBs and higher number of foci still present at 20 h post-irradiation, suggesting that DSB clusters within some megabasepairs of chromatin have a large impact on the repair. Recent data on γ-H2AX foci formation on rejoined chromosomes (Suzuki et al., 2006) might also indicate that late large γ-H2AX foci are a result of chromatin alteration after DNA rejoining. Thus, it is possible that some of the γ-H2AX foci remaining after 20 h post irradiation may also represent misrepair of DSBs.

2.5 GENERAL CONCLUSIONS

In connection to the use of radiation for cancer therapy, that is both efficient in killing the tumor cells and safe for the surrounding healthy tissues, more knowledge is needed on the mechanisms involved in the DNA damage induction and repair. To correctly estimate the cellular responses to DNA damage, it is crucial to accurately measure the number of DSB induced. Assessment of the DNA damage induction and the signaling response pathways are influenced by several biological, physical, as well as methodological aspects. In this thesis was shown that the quantification of DSB yields is influenced by the methodology used, radiation quality, chromatin structure and lysis temperature. In summary, the presented data demonstrate that DSB yields and distributions are greatly influenced by ionization density and chromatin compactness. Clustering of DSB and other DNA lesions may affect the reparability. Furthermore, the detection of protein activation in single cells after ion track irradiation suggested that chromatin changes or other signaling processes might take place at distance from DSB. The data presented in this thesis provide new insights on the importance of the chromatin organization and the repair of clustered damage sites, as well as the role of repair-associated proteins in DNA damage recognition after high-LET radiation.

2.6 FUTURE STUDIES

In relation to cancer radiotherapy, many aspects regarding the mechanisms involved in the induction and repair of DNA damage are still not fully understood. Identifying the steps by which the DNA repair-related proteins are activated in response to ionizing radiation, as well as the roles of DNA damage clustering and chromatin structure in the repair process, might provide critical information that may lead to development of more effective cancer treatment strategies in the future.

The DNA damage and repair processes are associated with the occurrence of repair foci and other modifications in the nuclear architecture, at the sites of DSBs and throughout the nucleus. The detailed investigation of a potential link between DNA damage response and the changes of the subnuclear domains, as well as the chromatin

disassembly and reassembly, may prove useful in elucidating the DNA repair mechanisms and in placing the cellular responses to DNA damage into a broader context. Moreover, the interplay between the chromatin disassembly/reassembly, cell cycle checkpoints and repair mechanisms in response to DNA damage, is not completely characterized.

In response to DSB induction, ATM protein kinase activates both cell cycle arrest and an end-processing pathway involved in the repair of a subset of highly complex DSBs, such are those induced by high-LET radiation. Thus, the track-related pATM foci that we found in high-LET irradiated cells (Paper IV) may represent complex DSBs that require ATM-Artemis-dependent pathway, and are slowly rejoined, gaining advantage of the ATM-dependent cell cycle arrest. Therefore, it would be of interest to further study the interaction between ATM-dependent signaling and NHEJ pathway in relation to high-LET induced DSBs. In addition, more knowledge on the repair of DSB of various complexities could be useful in recognizing particular subsets of critical DSBs.

3 ACKNOWLEDGEMENTS

This work was funded by grants from the Gustav Vth Jubilee Foundation, the Stockholm Cancer Society, the Swedish Cancer Society, and from the European Commission. The financial support is gratefully acknowledged.

The studies presented in this thesis were carried out at both the Karolinska Biomics Center, Department of Oncology-Pathology, Karolinska Institute and the Division of Biomedical Radiation Sciences, Uppsala University. Many people have contributed in various ways, and I would like to express my thanks to you all, especially to:

My main supervisor, *Professor Rolf Lewensohn*, for accepting me as a PhD student in his research group, for valuable scientific discussions, unfailing support and advice regarding my studies.

My co-supervisor, *Assoc. prof. Bo Stenerlöw*, for welcoming me in his lab when I first came to Sweden as an exchange student. I would like to express my sincere gratitude for invaluable guidance, continuous support, availability and scientific inspiration throughout the years. Thank you also for your encouragement to learn Swedish language. It made my life much easier here.

My co-supervisor, *Dr. Kristina Viktorsson*, for interesting discussions, constructive comments on our manuscript and for the nice company during the conference in Los Angeles.

Professor Jörgen Carlsson, for providing such an enjoyable working atmosphere at BMS and for general support.

My co-author and room-mate, *Karin Karlsson*, for very good collaboration throughout the years and for the nice company during the conference in Copenhagen.

My co-author *Kecke Elmroth*, for very good collaboration and for friendship.

My co-authors *Fredrik Qvarnström* and *Martin Simonsson* for the invaluable assistance with computer analysis of foci and for interesting discussions.

The staff at Theodore Svedberg Laboratory (TSL), Uppsala, for assistance with the accelerated ion beam experiments, especially *Torbjörn Hartman* for his help with ion beam measurements and dosimetry.

Jan Grawé for very useful technical assistance with the confocal microscope.

Fiona Murray for her kind help with the language corrections on Paper IV.

All members of BMS: *Nina, Lars, Åsa, Ann-Charlott, Mikael, Kalle, Marika, Ylva, Shirin, Amelie, Erika, Lina, Thuy, Sara A, Ulrika, Helena, Ann-Sofie, Hanna, Camilla,*

Sara H, for very pleasant company and for the fun parties. Special thanks to *Veronika Asplund* for all her care, cheerful spirit and readiness to render practical help whenever necessary.

Members of KBC, among others: *Jessica, Åsa, Anja, Janne, Maria, Sara, Helena, Luigi, Betszy, Dali, Lukas, Brigitta*, for friendly atmosphere and interesting discussions. Special thanks to *Marianne Langéen* for valuable assistance in all the administrative issues, and for sharing and caring.

The chairman of the Department of Oncology-Pathology, Karolinska Institute, *Tina Dalianis*, for creating a good working atmosphere.

Prof. Laura Tugulea and *Prof. emeritus Gunnar Tibell* for offering me the opportunity to be enrolled in a SOCRATES exchange programme and for mediating the connection with the host department at Uppsala University.

Dr. Daria Mihalache, from Victor Babes Institute, Bucharest, for support and encouragement.

My Swedish and international friends: *Ovidiu, Mihaela, Milena, Karin D, Marc and Stéphanie, Johanna and Erik, Anna and Vladimir, Anica D, Daria, Mia, Alina, Leila, Kebrom, Ulrike R, Sébastien, Wei,* for support, for all the fun and interesting discussions, for keeping me plugged into different realities of the world and for making my time in Sweden a memorable experience.

My sister *Cristina* and her family, for being so supportive and understanding of my need of doing studies and experiencing life far away from home.

Last but not least, my mother *Maria-Venera*, for the love, constant encouragement and positive spirit. *Mama*, your high level of determination in everything you do is an inspiration for me!

Thank you all!

4 REFERENCES

Abramoff, M.D., Magelhaes, P.J. and Ram, S.J. (2004) Image Processing with ImageJ. Biophoton. int., **11**, 36-42.

Adams, K.E., Medhurst, A.L., Dart, D.A. and Lakin, N.D. (2006) Recruitment of ATR to sites of ionising radiation-induced DNA damage requires ATM and components of the MRN protein complex. Oncogene, **13**, 13.

Ahnesorg, P., Smith, P. and Jackson, S.P. (2006) XLF interacts with the XRCC4-DNA ligase IV complex to promote DNA nonhomologous end-joining. Cell., **124**, 301-313.

Bakkenist, C.J. and Kastan, M.B. (2003) DNA damage activates ATM through intermolecular autophosphorylation and dimer dissociation. Nature, **421**, 499-506.

Bekker-Jensen, S., Lukas, C., Kitagawa, R., Melander, F., Kastan, M.B., Bartek, J. and Lukas, J. (2006) Spatial organization of the mammalian genome surveillance machinery in response to DNA strand breaks. J. Cell. Biol., **173**, 195-206.

Bekker-Jensen, S., Lukas, C., Melander, F., Bartek, J. and Lukas, J. (2005) Dynamic assembly and sustained retention of 53BP1 at the sites of DNA damage are controlled by Mdc1/NFBD1. J. Cell. Biol., **170**, 201-211.

Blocher, D. (1990) In CHEF electrophoresis a linear induction of dsb corresponds to a nonlinear fraction of extracted DNA with dose. Int. J. Radiat. Biol., **57**, 7-12.

Bree, R.T., Neary, C., Samali, A. and Lowndes, N.F. (2004) The switch from survival responses to apoptosis after chromosomal breaks. DNA Repair (Amst). **3**, 989-995.

Bryant, P.E. (1985) Enzymatic restriction of mammalian cell DNA: evidence for double-strand breaks as potentially lethal lesions. Int J Radiat Biol Relat Stud Phys Chem Med, **48**, 55-60.

Buck, D., Malivert, L., de Chasseval, R., Barraud, A., Fondaneche, M.C., Sanal, O., Plebani, A., Stephan, J.L., Hufnagel, M., le Deist, F., Fischer, A., Durandy, A., de Villartay, J.P. and Revy, P. (2006) Cernunnos, a novel nonhomologous end-joining factor, is mutated in human immunodeficiency with microcephaly. Cell., **124**, 287-299.

Budman, J., Kim, S.A. and Chu, G. (2007) Processing of DNA for nonhomologous end-joining is controlled by kinase activity and XRCC4/ligase IV. J Biol Chem., **282**, 11950-11959.

Burma, S., Chen, B.P. and Chen, D.J. (2006) Role of non-homologous end joining (NHEJ) in maintaining genomic integrity. DNA Repair, **3**, 3.

Burma, S., Chen, B.P., Murphy, M., Kurimasa, A. and Chen, D.J. (2001) ATM Phosphorylates Histone H2AX in Response to DNA Double-strand Breaks. J. Biol. Chem., **276**, 42462-42467.

Caldecott, K.W. (2003) XRCC1 and DNA strand break repair. DNA Repair (Amst). **2**, 955-969.

Capp, J.-P., Boudsocq, F., Bertrand, P., Laroche-Clary, A., Pourquier, P., Lopez, B.S., Cazaux, C., Hoffmann, J.-S. and Canitrot, Y. (2006) The DNA polymerase {lambda} is required for the repair of non-compatible DNA double strand breaks by NHEJ in mammalian cells. Nucl. Acids Res., **34**, 2998-3007.

Chai, B., Huang, J., Cairns, B.R. and Laurent, B.C. (2005) Distinct roles for the RSC and Swi/Snf ATP-dependent chromatin remodelers in DNA double-strand break repair. Genes Dev., **19**, 1656–1661.

Chan, D.W., Chen, B.P.-C., Prithivirajsingh, S., Kurimasa, A., Story, M.D., Qin, J. and Chen, D.J. (2002) Autophosphorylation of the DNA-dependent protein kinase catalytic subunit is required for rejoining of DNA double-strand breaks. Genes Dev., **16**, 2333-2338.

Chen, F., Peterson, S.R., Story, M.D. and Chen, D.J. (1996) Disruption of DNA-PK in Ku80 mutant xrs-6 and the implications in DNA double-strand break repair. Mutat Res, **362**, 9-19.

Cox, R., Thacker, J., Goodhead, D.T. and Munson, R.J. (1977) Mutation and inactivation of mammalian cells by various ionising radiations. Nature, **267**, 425-427.

Cucinotta, F.A., Nikjoo, H. and Goodhead, D.T. (2000) Model for radial dependence of frequency distributions for energy imparted in nanometer volumes from HZE particles. Radiat Res., **153**, 459-468.

Cui, X., Yu, Y., Gupta, S., Cho, Y.-M., Lees-Miller, S.P. and Meek, K. (2005) Autophosphorylation of DNA-Dependent Protein Kinase Regulates DNA End Processing and May Also Alter Double-Strand Break Repair Pathway Choice. Mol. Cell. Biol., **25**, 10842-10852.

Dahm-Daphi, J., Dikomey, E., Pyttlik, C. and Jeggo, P.A. (1993) Reparable and non-reparable DNA strand breaks induced by X-irradiation in CHO K1 cells and the radiosensitive mutants xrs1 and xrs5. Int J Radiat Biol., **64**, 19-26.

Dahm-Daphi, J., Sass, C. and Alberti, W. (2000) Comparison of biological effects of DNA damage induced by ionizing radiation and hydrogen peroxide in CHO cells. Int J Radiat Biol., **76**, 67-75.

DeFazio, L.G., Stansel, R.M., Griffith, J.D. and Chu, G. (2002) Synapsis of DNA ends by DNA-dependent protein kinase. EMBO J., **21**, 3192-3200.

Delacote, F., Han, M., Stamato, T.D., Jasin, M. and Lopez, B.S. (2002) An xrcc4 defect or Wortmannin stimulates homologous recombination specifically induced by double-strand breaks in mammalian cells. Nucl. Acids. Res., **30**, 3454-3463.

DiBiase, S.J., Zeng, Z.C., Chen, R., Hyslop, T., Curran, W.J., Jr. and Iliakis, G. (2000) DNA-dependent protein kinase stimulates an independently active, nonhomologous, end-joining apparatus. Cancer Res, **60**, 1245-1253.

Downs, J.A., Nussenzweig, M.C. and Nussenzweig, A. (2007) Chromatin dynamics and the preservation of genetic information. Nature., **447**, 951-958.

Dupre, A., Boyer-Chatenet, L. and Gautier, J. (2006) Two-step activation of ATM by DNA and the Mre11-Rad50-Nbs1 complex. Nat. Struct. Mol. Biol., **13**, 451-457.

Fernandez-Capetillo, O., Lee, A., Nussenzweig, M. and Nussenzweig, A. (2004) H2AX: the histone guardian of the genome. DNA Repair (Amst.), **3**, 959-967.

Filipski, J., Leblanc, J., Youdale, T., Sikorska, M. and Walker, P.R. (1990) Periodicity of DNA folding in higher order chromatin structures. EMBO J., **9**, 1319-1327.

Flaus, A., Martin, D.M., Barton, G.J. and Owen-Hughes, T. (2006) Identification of multiple distinct Snf2 subfamilies with conserved structural motifs. Nucleic Acids Res., **34**, 2887–2905.

Goodarzi, A.A., Yu, Y., Riballo, E., Douglas, P., Walker, S.A., Ye, R., Harer, C., Marchetti, C., Morrice, N., Jeggo, P.A. and Lees-Miller, S.P. (2006) DNA-PK autophosphorylation facilitates Artemis endonuclease activity. Embo J, **27**, 27.

Goodhead, D.T. (1989) The initial physical damage produced by ionizing radiations. Int J Radiat Biol., **56**, 623-634.

Goodhead, D.T. (1994) Initial events in the cellular effects of ionizing radiations: clustered damage in DNA. Int. J. Radiat. Biol., **65**, 7-17.

Gulston, M., de Lara, C., Jenner, T., Davis, E. and O'Neill, P. (2004) Processing of clustered DNA damage generates additional double-strand breaks in mammalian cells post-irradiation. Nucleic Acids Res, **32**, 1602-1609. Print 2004.

Hall, E.J. and Giaccia, A.J. (2006) Radiobiology for the Radiologist, 6th ed., Lippincott Williams & Wilkins, Philadelphia.

Hammarsten, O. and Chu, G. (1998) DNA-dependent protein kinase: DNA binding and activation in the absence of Ku. Proc Natl Acad Sci U S A, **95**, 525-530.

Hanahan, D. and Weinberg, R.A. (2000) The hallmarks of cancer. Cell., **100**, 57-70.

Hansen, J.C. (2002) Conformational dynamics of the chromatin fiber in solution: determinants, mechanisms, and functions. Annu. Rev. Biophys. Biomol. Struct., **31**, 361-392.

Hentges, P., Ahnesorg, P., Pitcher, R.S., Bruce, C.K., Kysela, B., Green, A.J., Bianchi, J., Wilson, T.E., Jackson, S.P. and Doherty, A.J. (2006) Evolutionary and functional conservation of the DNA non-homologous end-joining protein, XLF/Cernunnos. J Biol Chem., **281**, 37517-37526.

Hickson, I., Zhao, Y., Richardson, C.J., Green, S.J., Martin, N.M., Orr, A.I., Reaper, P.M., Jackson, S.P., Curtin, N.J. and Smith, G.C. (2004) Identification and characterization of a novel and specific inhibitor of the ataxia-telangiectasia mutated kinase ATM. Cancer Res., **64**, 9152-9159.

Hoglund, E., Blomquist, E., Carlsson, J. and Stenerlow, B. (2000) DNA damage induced by radiation of different linear energy transfer: initial fragmentation. Int. J. Radiat. Biol., **76**, 539-547.

Hoglund, H. and Stenerlow, B. (2001) Induction and rejoining of DNA double-strand breaks in normal human skin fibroblasts after exposure to radiation of different linear energy transfer: possible roles of track structure and chromatin organization. Radiat. Res., **155**, 818-825.

Horn, P.J. and Peterson, C.L. (2002) Molecular biology. Chromatin higher order folding--wrapping up transcription. Science., **297**, 1824-1827.

Huyen, Y., Zgheib, O., Ditullio, R.A.J., Gorgoulis, V.G., Zacharatos, P., Petty, T.J., Sheston, E.A., Mellert, H.S., Stavridi, E.S. and Halazonetis, T.D. (2004) Methylated lysine 79 of histone H3 targets 53BP1 to DNA double-strand breaks. Nature, **432**, 406-411.

Ito, T. (2007) Role of histone modification in chromatin dynamics. J Biochem (Tokyo). **141**, 609-614.

Jackson, D.A., Dickinson, P. and Cook, P.R. (1990) The size of chromatin loops in HeLa cells. EMBO J., **9**, 567-571.

Jakob, B., Scholz, M. and Taucher-Scholz, G. (2003) Biological imaging of heavy charged-particle tracks. Radiat. Res., **159**, 676-684.

Jeggo, P.A. and Lobrich, M. (2006) Contribution of DNA repair and cell cycle checkpoint arrest to the maintenance of genomic stability. DNA Repair (Amst.), **5**, 1192-1198.

Karlsson, K.H. and Stenerlow, B. (2004) Focus formation of DNA repair proteins in normal and repair-deficient cells irradiated with high-LET ions. Radiat. Res., **161**, 517-527.

Kastan, M.B. and Lim, D.S. (2000) The many substrates and functions of ATM. Nat. Rev. Mol. Cell. Biol., **1**, 179-186.

Keogh, M.C., Kim, J.A., Downey, M., Fillingham, J., Chowdhury, D., Harrison, J.C., Onishi, M., Datta, N., Galicia, S., Emili, A., Lieberman, J., Shen, X., Buratowski, S., Haber, J.E., Durocher, D., Greenblatt, J.F. and Krogan, N.J. (2006) A phosphatase complex that dephosphorylates gammaH2AX regulates DNA damage checkpoint recovery. Nature, **439**, 497-501.

Kim, J.-S., Krasieva, T.B., Kurumizaka, H., Chen, D.J., Taylor, A.M.R. and Yokomori, K. (2005) Independent and sequential recruitment of NHEJ and HR factors to DNA damage sites in mammalian cells. J. Cell Biol., **170**, 341-347.

Kobayashi, J., Tauchi, H., Sakamoto, S., Nakamura, A., Morishima, K., Matsuura, S., Kobayashi, T., Tamai, K., Tanimoto, K. and Komatsu, K. (2002) NBS1 Localizes to gamma-H2AX Foci through Interaction with the FHA/BRCT Domain. Curr. Biol., **12**, 1846-1851.

Kozlov, S.V., Graham, M.E., Peng, C., Chen, P., Robinson, P.J. and Lavin, M.F. (2006) Involvement of novel autophosphorylation sites in ATM activation. EMBO J., **25**, 3504-3514.

Krogh, B.O. and Symington, L.S. (2004) Recombination proteins in yeast. Annu Rev Genet., **38**, 233-271.

Kruhlak, M.J., Celeste, A., Dellaire, G., Fernandez-Capetillo, O., Muller, W.G., McNally, J.G., Bazett-Jones, D.P. and Nussenzweig, A. (2006a) Changes in chromatin structure and mobility in living cells at sites of DNA double-strand breaks. J. Cell Biol., **172**, 823-834.

Kruhlak, M.J., Celeste, A. and Nussenzweig, A. (2006b) Spatio-temporal dynamics of chromatin containing DNA breaks. Cell Cycle, **5**, 1910-1912.

Kuhne, M., Rothkamm, K. and Lobrich, M. (2000) No dose-dependence of DNA double-strand break misrejoining following alpha-particle irradiation. Int J Radiat Biol., **74**, 891-900.

Kurz, E.U. and Lees-Miller, S.P. (2004) DNA damage-induced activation of ATM and ATM-dependent signaling pathways. DNA Repair (Amst.), **3**, 889-900.

Kwon, Y., Chi, P., Roh, D.H., Klein, H. and Sung, P. (2007) Synergistic action of the Saccharomyces cerevisiae homologous recombination factors Rad54 and Rad51 in chromatin remodeling. DNA Repair (Amst). **6**, 1496-1506.

Lavin, M.F. (2004) The Mre11 complex and ATM: a two-way functional interaction in recognising and signaling DNA double strand breaks. DNA Repair (Amst.), **3**, 1515-1520.

Leatherbarrow, E.L., Harper, J.V., Cucinotta, F.A. and O'Neill, P. (2006) Induction and quantification of gamma-H2AX foci following low and high LET-irradiation. Int J Radiat Biol., **82**, 111-118.

Lee, J.H. and Paull, T.T. (2005) ATM Activation by DNA Double-Strand Breaks Through the Mre11-Rad50-Nbs1 Complex. Science, **24**, 24.

Ljungman, M. (1990) The role of chromatin in the induction and repair of DNA damage, in Department of Radiobiology. Stockholm University: Stockholm., 18.

Ljungman, M. (1991) The influence of chromatin structure on the frequency of radiation-induced DNA strand breaks: A study using nuclear and nucleoid monolayers. Radiat. Res., **126**, 58-64.

Lobrich, M., Cooper, P.K. and Rydberg, B. (1996) Non-random distribution of DNA double-strand breaks induced by particle irradiation. Int. J. Radiat. Biol., **70**, 493-503.

Lobrich, M., Cooper, P.K. and Rydberg, B. (1998) Joining of correct and incorrect DNA ends at double-strand breaks produced by high-linear energy transfer radiation in human fibroblasts. Radiat Res, **150**, 619-626.

Lou, Z., Minter-Dykhouse, K., Franco, S., Gostissa, M., Rivera, M.A., Celeste, A., Manis, J.P., van Deursen, J., Nussenzweig, A., Paull, T.T., Alt, F.W. and Chen, J. (2006) MDC1 maintains genomic stability by participating in the amplification of ATM-dependent DNA damage signals. Mol. Cell., **21**, 187-200.

Luger, K., Mader, A.W., Richmond, R.K., Sargent, D.F. and Richmond, T.J. (1997) Crystal structure of the nucleosome core particle at 2.8 A resolution. Nature., **389**, 251-260.

Lundin, C., Erixon, K., Arnaudeau, C., Schultz, N., Jenssen, D., Meuth, M. and Helleday, T. (2002) Different roles for nonhomologous end joining and homologous recombination following replication arrest in mammalian cells. Mol Cell Biol., **22**, 5869-5878.

Ma, Y., Pannicke, U., Schwarz, K. and Lieber, M.R. (2002) Hairpin opening and overhang processing by an Artemis/DNA-dependent protein kinase complex in nonhomologous end joining and V(D)J recombination. Cell, **108**, 781-794.

MacPhail, S.H., Banath, J.P., Yu, T.Y., Chu, E.H., Lambur, H. and Olive, P.L. (2003) Expression of phosphorylated histone H2AX in cultured cell lines following exposure to X-rays. Int J Radiat Biol, **79**, 351-358.

Mahajan, K.N., Nick McElhinny, S.A., Mitchell, B.S. and Ramsden, D.A. (2002) Association of DNA polymerase mu (pol mu) with Ku and ligase IV: role for pol mu in end-joining double-strand break repair. Mol Cell Biol., **22**, 5194-5202.

Malyarchuk, S., Brame, K.L., Youngblood, R., Shi, R. and Harrison, L. (2004) Two clustered 8-oxo-7,8-dihydroguanine (8-oxodG) lesions increase the point mutation frequency of 8-oxodG, but do not result in double strand breaks or deletions in Escherichia coli. Nucleic Acids Res., **32**, 5721–5731.

Newman, H.C., Prise, K.M., Folkard, M. and Michael, B.D. (1997) DNA double-strand break distributions in X-ray and alpha-particle irradiated V79 cells: evidence for non-random breakage. Int J Radiat Biol., **71**, 347-363.

Newman, H.C., Prise, K.M. and Michael, B.D. (2000) The role of higher-order chromatin structure in the yield and distribution of DNA double-strand breaks in cells irradiated with X-ray or alpha-particle. Int J Radiat Biol., **76**, 1085-1093.

Nygren, J., Ljungman, M. and Ahnstrom, G. (1995) Chromatin structure and radiation-induced DNA strand breaks in human cells: Soluble scavengers and DNA-

bound proteins offer a better protection against single- than double-strand breaks. Int J Radiat Biol., **68**, 11-18.

Oleinick, N.L. and Chiu, S.-M. (1994) Nuclear and chromatin structures and their influence on the radiosensitivity of DNA. Radiat Prot Dosimetry., **52**, 353-358.

Olsson, G., Czene, S., Jenssen, D. and Harms-Ringdahl, M. (2004) Induction of homologous recombination in the hprt gene of V79 Chinese hamster cells in response to low- and high-LET irradiation. Cytogenet Genome Res., **104**, 227-231.

Parseghian, M.H. and Hamkalo, B.A. (2001) A compendium of the histone H1 family of somatic subtypes: an elusive cast of characters and their characteristics. Biochem Cell Biol., **79**, 289-304.

Paull, T.T., Rogakou, E.P., Yamazaki, V., Kirchgessner, C.U., Gellert, M. and Bonner, W.M. (2000) A critical role for histone H2AX in recruitment of repair factors to nuclear foci after DNA damage. Curr. Biol., **10**, 886-895.

Pinto, M., Prise, K.M. and Michael, B.D. (2005) Evidence for complexity at the nanometer scale of radiation-induced DNA DSBs as a determinant of rejoining kinetics. Radiat. Res., **164**, 73–85.

Potter, A.J., Gollahon, K.A., Palanca, B.J.A., Harbert, M.J., Choi, Y.M., Moskovitz, A.H., Potter, J.D. and Rabinovitch, P.S. (2002) Flow cytometric analysis of the cell cycle phase specificity of DNA damage induced by radiation, hydrogen peroxide and doxorubicin. Carcinogenesis, **23**, 389-401.

Qvarnstrom, O.F., Simonsson, M., Johansson, K.A., Nyman, J. and Turesson, I. (2004) DNA double strand break quantification in skin biopsies. Radiother. Oncol., **72**, 311-317.

Ramakrishnan, V. (1997) Histone H1 and chromatin higher-order structure. Crit Rev Eukaryot Gene Expr., **7**, 215-230.

Reddy, Y.V.R., Ding, Q., Lees-Miller, S.P., Meek, K. and Ramsden, D.A. (2004) Non-homologous End Joining Requires That the DNA-PK Complex Undergo an Autophosphorylation-dependent Rearrangement at DNA Ends. J. Biol. Chem., **279**, 39408-39413.

Riballo, E., Kuhne, M., Rief, N., Doherty, A., Smith, G.C., Recio, M.J., Reis, C., Dahm, K., Fricke, A., Krempler, A., Parker, A.R., Jackson, S.P., Gennery, A., Jeggo, P.A. and Lobrich, M. (2004) A Pathway of Double-Strand Break Rejoining Dependent upon ATM, Artemis, and Proteins Locating to gamma-H2AX Foci. Mol. Cell, **16**, 715-724.

Rogakou, E.P., Boon, C., Redon, C. and Bonner, W.M. (1999) Megabase chromatin domains involved in DNA double-strand breaks in vivo. J Cell Biol, **146**, 905-916.

Rogakou, E.P., Pilch, D.R., Orr, A.H., Ivanova, V.S. and Bonner, W.M. (1998) DNA double-stranded breaks induce histone H2AX phosphorylation on serine 139. J. Biol. Chem., **273**, 5858-5868.

Rothkamm, K., Kruger, I., Thompson, L.H. and Lobrich, M. (2003) Pathways of DNA Double-Strand Break Repair during the Mammalian Cell Cycle. Mol. Cell. Biol., **23**, 5706-5715.

Rouse, J. and Jackson, S.P. (2002) Interfaces Between the Detection, Signaling, and Repair of DNA Damage. Science, **297**, 547-551.

Rydberg, B. (1996) Clusters of DNA damage induced by ionizing radiation: formation of short DNA fragments. II. Experimental detection. Radiat. Res., **145**, 200-209.

Rydberg, B. (2000) Radiation-induced heat-labile sites that convert into DNA double-strand breaks. Radiat Res, **153**, 805-812.

Rydberg, B. (2001) Radiation induced DNA damage and chromatin structure. Acta Oncol., **40**, 682-685.

Sachs, R.K., van den Engh, G., Trask, B., Yokota, H. and Hearst, J.E. (1995) A random-walk/giant-loop model for interphase chromosomes. Proc Natl Acad Sci U S A, **92**, 2710-2714.

Saintigny, Y., Delacôte, F., Boucher, D., Averbeck, D. and Lopez, B.S. (2007) XRCC4 in G1 suppresses homologous recombination in S/G2, in G1 checkpoint-defective cells. Oncogene., **26**, 2769-2780.

Schultz, L.B., Chehab, N.H., Malikzay, A. and Halazonetis, T.D. (2000) p53 Binding Protein 1 (53BP1) Is an Early Participant in the Cellular Response to DNA Double-Strand Breaks. J. Cell Biol., **151**, 1381-1390.

Shiloh, Y. (2006) The ATM-mediated DNA-damage response: taking shape. Trends Biochem. Sci., **31**, 402-410.

Shim, E.Y., Hong, S.J., Oum, J.H., Yanez, Y., Zhang, Y. and Lee, S.E. (2007) RSC mobilizes nucleosomes to improve accessibility of repair machinery to the damaged chromatin. Mol Cell Biol., **27**, 1602-1613.

Singleton, B.K., Griffin, C.S. and Thacker, J. (2002) Clustered DNA Damage Leads to Complex Genetic Changes in Irradiated Human Cells. Cancer Res, **62**, 6263-6269.

Smits, V.A., Reaper, P.M. and Jackson, S.P. (2006) Rapid PIKK-dependent release of Chk1 from chromatin promotes the DNA-damage checkpoint response. Curr. Biol., **16**, 150-159.

Sonka, M., Hlavac, V. and Boyle, R. (1998) Image processing, analysis, and machine vision (2nd edn), Pacific Grove, California.

Stenerlow, B., Blomquist, E., Grusell, E., Hartman, T. and Carlsson, J. (1996) Rejoining of DNA double-strand breaks induced by accelerated nitrogen ions. Int J Radiat Biol., **70**, 413-420.

Stenerlow, B. and Hoglund, E. (2002) Rejoining of double-stranded DNA-fragments studied in different size-intervals. Int. J. Radiat. Biol., **78**, 1-7.

Stenerlow, B., Hoglund, E., Carlsson, J. and Blomquist, E. (2000) Rejoining of DNA fragments produced by radiations of different linear energy transfer. Int. J. Radiat. Biol., **76**, 549-557.

Stenerlow, B., Karlsson, K.H., Cooper, B. and Rydberg, B. (2003) Measurement of prompt DNA double-strand breaks in mammalian cells without including heat-labile sites: results for cells deficient in nonhomologous end joining. Radiat. Res., **159**, 502-510.

Stiff, T., O'Driscoll, M., Rief, N., Iwabuchi, K., Lobrich, M. and Jeggo, P.A. (2004) ATM and DNA-PK function redundantly to phosphorylate H2AX after exposure to ionizing radiation. Cancer Res., **64**, 2390-2396.

Stucki, M., Clapperton, J.A., Mohammad, D., Yaffe, M.B., Smerdon, S.J. and Jackson, S.P. (2005) MDC1 Directly Binds Phosphorylated Histone H2AX to Regulate Cellular Responses to DNA Double-Strand Breaks. Cell, **123**, 1213-1226.

Stucki, M. and Jackson, S.P. (2006) gammaH2AX and MDC1: Anchoring the DNA-damage-response machinery to broken chromosomes. DNA Repair, **5**, 534-543.

Suzuki, M., Suzuki, K., Kodama, S. and Watanabe, M. (2006) Phosphorylated histone H2AX foci persist on rejoined mitotic chromosomes in normal human diploid cells exposed to ionizing radiation. Radiat. Res., **165**, 269-276.

Uziel, T., Lerenthal, Y., Moyal, L., Andegeko, Y., Mittelman, L. and Shiloh, Y. (2003) Requirement of the MRN complex for ATM activation by DNA damage. EMBO J., **22**, 5612-5621.

van Dyck, E., Stasiak, A.Z., Stasiak, A. and West, S.C. (1999) Binding of double-strand breaks in DNA by human Rad52 protein. Nature, **398**, 728-731.

Walker, J.R., Corpina, R.A. and Goldberg, J. (2001) Structure of the Ku heterodimer bound to DNA and its implications for double-strand break repair. Nature, **412**, 607-614.

Wang, H., Zeng, Z.C., Bui, T.A., Sonoda, E., Takata, M., Takeda, S. and Iliakis, G. (2001) Efficient rejoining of radiation-induced DNA double-strand breaks in vertebrate cells deficient in genes of the RAD52 epistasis group. Oncogene, **20**, 2212-2224.

Ward, J.F. (1988) DNA damage produced by ionizing radiation in mammalian cells: identities, mechanisms of formation, and reparability. Prog Nucleic Acid Res Mol Biol., **35**, 95-125.

Weterings, E. and van Gent, D.C. (2004) The mechanism of non-homologous end-joining: a synopsis of synapsis. DNA Repair (Amst). **3**, 1425-1435.

Wu, P.Y., Frit, P., Malivert, L., Révy, P., Biard, D., Salles, B. and Calsou, P. (2007) Interplay between cernunnos-XLF and NHEJ proteins at DNA ends in the cell. J Biol Chem.

Wyman, C., Ristic, D. and Kanaar, R. (2004) Homologous recombination-mediated double-strand break repair. DNA Repair (Amst). **3**, 827-833.

Yoo, S. and Dynan, W.S. (1999) Geometry of a complex formed by double strand break repair proteins at a single DNA end: recruitment of DNA-PKcs induces inward translocation of Ku protein. Nucleic Acids Res, **27**, 4679-4686.

You, Z., Chahwan, C., Bailis, J., Hunter, T. and Russell, P. (2005) ATM activation and its recruitment to damaged DNA require binding to the C terminus of Nbs1. Mol Cell Biol., **25**, 5363-5379.

Zhou, B.B. and Elledge, S.J. (2000) The DNA damage response: putting checkpoints in perspective. Nature, **408**, 433-439.

Ziv, Y., Bielopolski, D., Galanty, Y., Lukas, C., Taya, Y., Schultz, D.C., Lukas, J., Bekker-Jensen, S., Bartek, J. and Shiloh, Y. (2006) Chromatin relaxation in response to DNA double-strand breaks is modulated by a novel ATM and KAP-1 dependent pathway. Nat. Cell. Biol., **8**, 870-876.